CO₂-equivalence metrics for surface albedo change based on the radiative forcing concept: A critical review

Ryan M. Bright[1] and Marianne T. Lund[2]

[1]Department of Forest and Climate, Norwegian Institute of Bioeconomy Research (NIBIO), PO Box 115, 1431-Ås, Norway
[2]Centre for International Climate Research (CICERO), 0349 Oslo, Norway

Correspondence to: Ryan M. Bright (ryan.bright@nibio.no)

Abstract. Management of Earth's surface albedo is increasingly viewed as an important climate change mitigation strategy both on (Seneviratne et al., 2018) and off (Field et al., 2018;Kravitz et al., 2018) the land. Assessing the impact of a surface albedo change involves employing a measure like radiative forcing (*RF*) which can be challenging to digest for decision-makers who deal in the currency of CO_2-equivalent emissions. As a result, many researchers express albedo change ($\Delta\alpha$) *RF*s in terms of their CO_2-equivalent effects, despite the lack of a standard method for doing so, such as there is for emissions of well-mixed greenhouse gases (WMGHGs; e.g., IPCC AR5, Myhre et al. (2013)). A major challenge for converting $\Delta\alpha$ *RF*s into their "CO_2-equivalent" effects in a manner consistent with current IPCC emission metric approaches stems from the lack of a universal time-dependency following the perturbation (perturbation "lifetime"). Here, we review existing methodologies based on the *RF* concept with the goal of highlighting the context(s) in which the resulting CO_2-equivalent metrics may or may not have merit. To our knowledge this is the first review dedicated entirely to the topic since the first CO_2-eq. metric for $\Delta\alpha$ surfaced 20 years ago. We find that, although there are some methods that sufficiently address the time-dependency issue, none address or sufficiently account for the spatial disparity between the climate response to CO_2 emissions and $\Delta\alpha$ – a major critique of $\Delta\alpha$ metrics based on the *RF* concept (Jones et al., 2013). We conclude that considerable research efforts are needed to build consensus surrounding the *RF* "efficacy" of various surface forcing types associated with $\Delta\alpha$ (e.g., crop change, forest harvest, etc.), and the degree to which these are sensitive to the spatial pattern, extent, and magnitude of the underlying surface forcings.

1 Introduction

The albedo at Earth's surface helps to govern the amount of solar energy absorbed by the earth system and is thus a relevant physical property shaping weather and climate (Cess, 1978;Hansen et al., 1984;Pielke Sr. et al., 1998). On average, Earth reflects about 30% of the energy it receives from the sun, of which about 13% may be attributed to the surface albedo (Stephens et al., 2015;Donohoe and Battisti, 2011). In recent years it has become the subject of increasing research interest amongst the scientific community, as measures to increase Earth's surface albedo are increasingly viewed as an integral component of climate change mitigation and adaptation, both on (Seneviratne et al., 2018) and off (Field et al., 2018;Kravitz et al., 2018) the

30 land. Surface albedo modifications associated with large-scale carbon dioxide removal (CDR) like re-/afforestation can detract from the effectiveness of such mitigation strategies (Boysen et al., 2016), given that such modifications generally serve to increase Earth's solar radiation budget resulting in warming. Like emissions of GHGs and aerosols, perturbations to the planetary albedo via perturbations to the surface albedo represent true external forcings of the climate system and can be measured in terms of changes to Earth's radiative balance – or radiative forcings (Houghton et al., 1995). The radiative forcing

35 (RF) concept provides a first-order means to compare surface albedo changes (henceforth $\Delta\alpha$) to other perturbation types, thus enabling a more comprehensive evaluation of human activities altering Earth's surface (Houghton et al., 1995;Pielke Sr. et al., 2002).

Radiative forcing is a standard measure of the effects of various emissions or perturbations on climate, and can be used to

40 compare the effect of changes between any two points in time. It isa backward-looking measure accounting for the impact up to the given point anddoes not express the actual temperature response to the perturbation. To enable aggregation of emissions of different gases to a common scale, the concept of CO_2-equivalent emissions is commonly used in assessments, decision making, and policy frameworks. While initially introduced to illustrate the difficulties related to comparing the climate impacts of different gases, the field of emission metrics -- i.e., the methods to convert non-CO_2 radiative constituents into their CO_2-

45 equivalent effects – has evolved and presently includes a suite of alternative formulations, including the Global Warming Potential (GWP) adopted by the UNFCCC (O'Neill, 2000;Fuglestvedt et al., 2003;Fuglestvedt et al., 2010). Today, CO_2-equivalency metrics form an integral part of UNFCC emission reporting and climate agreements (e.g. The Kyoto Protocol) – in addition to the fields of Life Cycle Assessment (Heijungs and Guineév, 2012) and Integrated Assessment Modeling (O'Neill et al., 2016) – despite much debate around GWP as the metric of choice (Denison et al., 2019). As such, many researchers

50 seek to convert RF from $\Delta\alpha$ into a CO_2-equivalent effect, which is particularly useful in land use forcing research when perturbations to terrestrial carbon cycling often accompany the $\Delta\alpha$. Although seemingly straight-forward at the surface, the procedure is complicated by two key fundamental differences between $\Delta\alpha$ and CO_2: additional CO_2 becomes well-mixed within the atmosphere upon emission, and, the resulting atmospheric perturbation persists over millennia and cannot be fully reversed by human interventions. In other words, CO_2's RF is both temporally- and spatially-extensive with the ensuring

55 climate response being independent of the location of emission, whereas the RF and ensuing climate response following $\Delta\alpha$ is more localized and can be fully reversed on short time scales.

These challenges have led researchers to adapt a variety of diverging methods for converting albedo-change RFs (henceforth $RF_{\Delta\alpha}$) into CO_2-equivalence. Unlike for conventional GHGs, however, there has been little concerted effort by the climate

60 metric science community to build consensus or formalize a standard methodology for $RF_{\Delta\alpha}$ (as evidenced by IPCC AR4 and AR5). Here, we review existing CO_2-equivalent metrics for $\Delta\alpha$ and their underlying methods based on the RF concept. To our knowledge this is the first review dedicated to the topic since the first $\Delta\alpha$ metric surfaced 20 years ago. Herein, we compare and contrast existing metrics both quantitatively and qualitatively, with the main goal of providing added clarity surrounding

the context in which the proposed metrics have (de)merits.   We start in Section 2 by providing an overview of the methods
conventionally applied in the climate metric context for estimating radiative forcings following CO_2 emissions and surface
albedo change. We then present the reviewed $\Delta\alpha$ metrics in Section 3 and systematically evaluate them quantitatively in
Section 4 and qualitatively in Section 5. In Section 6 we review and evaluate a relatively new usage of the GWP metric
previously unapplied as a $\Delta\alpha$ metric – termed *GWP** -- while in Section 7 we review the interpretation challenges of a CO_2-
eq. measure for $\Delta\alpha$ based on the *RF* concept.   We conclude in Section 8 with a discussion about the limitations and
uncertainties of the reviewed metrics, while providing recommendations and guidance for future application.

2 Radiative forcings from CO_2 emissions and surface albedo change

IPCC emission metrics are based on the stratospherically-adjusted *RF* at the tropopause in which the stratosphere is allowed
to relax to the thermal steady state (Myhre et al., 2013;IPCC, 2001). Estimates of the stratospheric *RF* for CO_2 (henceforth
RF_{CO_2}) are derived from atmospheric concentration changes imposed in global radiative transfer models (Myhre et al.,
1998;Etminan et al., 2016). For shortwave *RF*s there is no evidence to suggest that the stratospheric temperature adjusts to a
surface albedo change (at least for land-use and land cover change (LULCC), Smith et al. (2020); Hansen et al., (2005); Huang
et al. (2020)) and thus the instantaneous shortwave flux change at TOA is typically taken as $RF_{\Delta\alpha}$, consistent with Myhre et
al. (2013).

One of the major critiques of the instantaneous or stratospherically-adjusted *RF* is that they may be inadequate as predictors
of the climate response (i.e., changes to near surface air temperatures, precipitation, etc.). The climate may respond differently
to different perturbation types despite similar *RF* magnitudes – or in other words – feedbacks are not independent of the
perturbation type (Hansen et al., 1997;Joshi et al., 2003). Alternative *RF* definitions that include tropospheric adjustments
(Shine et al., 2003) or even land surface temperature adjustments (Hansen et al., 2005) have been proposed with the argument
that such adjustments are more indicative of the type and magnitude of feedbacks underlying the climate response (Sherwood
et al., 2015;Myhre et al., 2013).   These alternatives – referred to as "effective radiative forcings (*ERF*)" – may be preferred
when they differ notably from the instantaneous- or stratospherically-adjusted *RF*, in which case their use might be preferred
in metric calculations. Alternatively, climate "efficacies" can be applied to adjust instantaneous or stratospherically-adjusted
RF – where efficacy is defined as the temperature response to some perturbation type relative to that of CO_2. The implications
of applying efficacies for spatially heterogenous perturbations like $\Delta\alpha$ are discussed further in Section 6.

2.1 CO_2 radiative forcings

Simplified expressions for the global mean RF_{CO_2} (in W m^{-2}) due to a perturbation to the atmospheric CO_2 concentration are
based on curve fits of radiative transfer model outputs (Myhre et al., 1998;Myhre et al., 2013) :

95 $$RF_{CO_2}(\Delta C) = 5.35\,ln\left(\frac{C_0 + \Delta C}{C_0}\right)$$ (1)

where C_0 is the initial concentration and ΔC is the concentration change. Because of the logarithmic relationship between RF and CO_2 concentration, CO_2's radiative efficiency – or the radiative forcing per unit change in concentration over a given background concentration – decreases with increasing background concentrations. When ΔC is 1 ppm and C_0 is the current

100 concentration, we may then refer to the solution of Eq. (1) as CO_2's current global mean radiative efficiency – or α_{CO_2} (in W m^{-2} ppm^{-1}).

Updates to the RF_{CO_2} function (Eq. 1) were given in Etminan et al. (2016) where the constant 5.35 (or $RF_{2\times CO_2}$/ln[2]) was replaced by an explicit function of CO_2, CH_4, and N_2O concentrations. However, this update is only important for very large

105 CO_2 perturbations and is unnecessary to consider for emission metrics that utilize radiative efficiencies for small perturbations around present-day concentrations (Etminan et al., 2016).

For emission metrics, it is more convenient to express CO_2's radiative efficiency in terms a mass-based concentration increase:

110 $$k_{CO_2} = \frac{\alpha_{CO_2}\varepsilon_{air}10^6}{\varepsilon_{CO_2}M_{atm}}$$ (2)

where α_{CO_2} is the radiative efficiency per 1 ppm concentration increase, ε_{CO_2} is the molecular weight of CO_2 (44.01 kg kmol^{-1}), ε_{air} is the molecular weight of air (28.97 kg kmol^{-1}), and M_{atm} is the mass of the atmosphere (5.14×10^{18} kg). The solution of Eq. (2) thus yields CO_2's global mean radiative efficiency with units in W m^{-2} kg^{-1}.

115

The global mean radiative forcing over time following a 1 kg pulse emission of CO_2 can be estimated with an impulse-response function describing atmospheric CO_2 removal in time by Earth's ocean and terrestrial CO2 sinks:

$$RF_{CO_2}(t) = k_{CO_2}\int_{t=0}^{t} y_{CO_2}(t)dt$$ (3)

120

where y_{CO_2} is a model describing the decay of CO_2 in the atmosphere over time. In AR5 y_{CO_2} is based on the multi-model mean CO_2 impulse-response function described in (Joos et al., 2013;Myhre et al., 2013) for a CO_2 background concentration of 389 ppmv, t is the time step, and k_{CO_2} is the radiative efficiency per kg CO_2 emitted upon the same background concentration (i.e., 1.76×10^{-15} W m^{-2} kg^{-1}) which is assumed constant and time-invariant for small perturbations and for the calculation of

125 emission metrics (Joos et al., 2013;Myhre et al., 2013). The pulse-response function (y_{CO_2}) comprises four carbon pools representing the combined effect of several carbon-cycle mechanisms rather than directly corresponding to individual physical

processes. Although considered ideal for metric calculations in IPCC AR5, state-dependent alternatives exist in which the carbon cycle response is affected by rising temperature or CO_2 accumulation in the atmosphere (Millar et al., 2017).

130   For an emission (or removal) scenario, $RF_{CO_2}(t)$ is estimated from changes to atmospheric CO_2 abundance computed as a convolution integral between emissions (or removals) and the CO_2 impulse-response function:

$$RF_{CO_2}(t) = k_{CO_2} \int_{t'=0}^{t} e(t') y_{CO_2}(t - t') dt' \tag{4}$$

135   where t is the time dimension, t' is the integration variable, $e(t')$ is the CO_2 emission (or removal) rate (in kg).

2.2 Shortwave radiative forcings from surface albedo change

The time step of Eq. (3) is typically one year, thus it is convenient to utilize an annually averaged $RF_{\Delta\alpha}$ when deriving a CO_2-equivalent metric. Given the asymmetry between solar irradiance and the seasonal cycle of surface albedo in many extra-tropical regions, a more precise estimate of the annual $RF_{\Delta\alpha}$ is one based on the monthly (or even daily) $\Delta\alpha$ (Bernier et al.,
140   2011).

The local annual mean instantaneous $RF_{\Delta\alpha}$ (in W m^{-2}) following monthly surface albedo changes (unitless) can be estimated with radiative kernels derived from global climate models [e.g., (Soden et al., 2008;Pendergrass et al., 2018;Block and Mauritsen, 2014;Smith et al., 2018)], although it should be pointed out that kernels are model- and state-dependent. Bright &
145   O'Halloran (2019) recently presented a simplified $RF_{\Delta\alpha}$ model allowing greater flexibility surrounding the prescribed atmospheric state, given as:

$$RF_{\Delta\alpha}(t) = \frac{1}{12} \sum_{m=1}^{12} -SW_{\downarrow,m,t}^{sfc} \sqrt{T_{m,t}} \Delta\alpha_{m,t} \tag{5}$$

150   where $\Delta\alpha_{m,t}$ is a surface albedo change in month m and year t, $SW_{\downarrow}^{sfc}$ is the incoming solar radiation flux incident at surface level in month m and year t, and $T_{m,t}$ is the all-sky monthly mean clearness index (or $SW_{\downarrow}^{sfc}/SW_{\downarrow}^{toa}$; unitless) in month m and year t.

It is important to reiterate that the $RF_{\Delta\alpha}$ defined with either Eq. (5) or GCM-based kernels strictly represents the instantaneous
155   shortwave flux change at TOA and is not directly comparable to other definitions of RF based on net (downward) radiative flux changes at TOA following atmospheric adjustments. A perturbation to $\Delta\alpha$ will result in a modification to the turbulent heat fluxes leading to radiative adjustments in the troposphere (Laguë et al., 2019;Huang et al., 2020;Chen and Dirmeyer,

2020). However, in the context of emission metrics, both $RF_{\Delta\alpha}$ and RF_{CO_2} have merit given that they do not require coupled climate model runs of several years to compute.

3 Overview of CO₂-equivalent metrics for $RF_{\Delta\alpha}$

Over the past 20 years, a variety of metrics and their permutations have been employed to express $RF_{\Delta\alpha}$ as "CO₂-equivalence", as evidenced from the 27 studies included in this review (Table 1).

Table 1. Studies included in this review.

Study	Metric	Notes
Betts (2000)	*EESF*	AF = 0.5
Akbari et al. (2009)	*EESF*	AF = 0.55
Montenegro et al. (2009)	*EESF*	AF = 0.5
Thompson et al. (2009a)	*EESF*	AF = 0.5
Thompson et al. (2009b)	*EESF*	AF = 0.5
Muñoz et al. (2010)	*EESF*	AF based on C-cycle model and *TH* = 20, 100, and 500 yrs.
Menon et al. (2010)	*EESF*	AF = 0.55
Georgscu et al. (2011)	*EESF*	AF = 0.50
Cherubini et al. (2012)	*GWP*	Based on effective *RF* estimated with a climate efficacy of 1.94[b]
Bright et al. (2012)	*GWP*	TH = 20; 100; 500 yrs.
Susca, T. (2012b)	$\sum$*TDEE*[a]	
Susca, T. (2012a)	$\sum$*TDEE*[a]	
Guest et al. (2013)	*GWP*	
Zhao & Jackson (2014)	*EESF*	AF = 0.5; Based on effective *RF* estimated with a climate efficacy of 0.52[c]
Caiazzo et al. (2014)	*EESF*	AF based on C-cycle model and *TH* = 100 yrs.
Singh et al. (2014)	*GWP*	TH = 100 yrs.
Bright et al. (2016)	*TDEE*; $\sum$*TDEE*	
Mykleby et al. (2017)	*EESF*	AF based on C-cycle model and *TH* = 80 yrs.
Fortier et al. (2017)	*EESF*	AF based on C-cycle model and *TH* = 100 yrs.
Carrer et al. (2018)	*EESF/TH*	AF based on C-cycle model and *TH* = 100 yrs.
Carrer et al. (2018)	*GWP/TH*	TH = 100 yrs.

Favero et al. (2018)	EESF	AF based on C-cycle model and TH = 100 yrs.
Sieber et al. (2019)	GWP	TH = 100 yrs.
Sieber et al. (2020)	GWP	TH = 100 yrs.
Genesio et al. (2020)	EESF	AF = 0.47
Sciusco et al. (2020)	EESF/TH	AF based on C-cycle model and TH = 100 yrs.
Bright et al. (2020)	TDEE; ∑TDEE	
Lugato et al. (2020)	GWP	TH = 84 yrs.

[a] Referred to as "time-dependent emission"; [b] From idealized climate model simulations of high Arctic snow albedo change (Bellouin and Boucher, 2010); [c] From idealized climate model simulations of global LULCC (Davin et al., 2007)

Chiefly differentiating the methods behind the metrics shown in Table 1 – described henceforth – is how time is represented with respect to both the $\Delta\alpha$ and the reference gas (i.e., CO2) perturbations. Among the most common approaches is to relate $RF_{\Delta\alpha}$ to the RF following a CO_2 emission imposed on some atmospheric CO_2 concentration background, but with a fraction of the emission instantaneously removed by Earth's ocean and terrestrial CO_2 sinks by an amount defined by one minus the so-called "airborne fraction" (AF) – or the growth in atmospheric CO_2 relative to anthropogenic CO_2 emissions (Forster et al., 2007).

This method – or the "emissions equivalent of shortwave forcing (*EESF*)" – was first introduced by Betts (2000) and may be expressed (in kg CO_2-eq. m^{-2}) as:

$$EESF = \frac{RF_{\Delta\alpha}}{k_{CO_2} A_E AF} \tag{6}$$

where $RF_{\Delta\alpha}$ is the local annual mean instantaneous RF from a prescribed monthly $\Delta\alpha$ scenario (in W m^{-2}), k_{CO_2} is the global mean radiative efficiency of CO_2 (e.g., Eq. (2); in W m^{-2} kg^{-1}), A_E is Earth's surface area (5.1×10^{14} m^2), and AF is the airborne fraction. Because AF appears in the denominator in Eq. (6), the CO_2 equivalent estimate will be highly sensitive to the choice of AF. Figure 1 plots AF since 1959 which, as can be seen, can fluctuate considerably over short time periods, ranging from a high of 0.81 in 1987 and low of 0.20 in 1992.

185
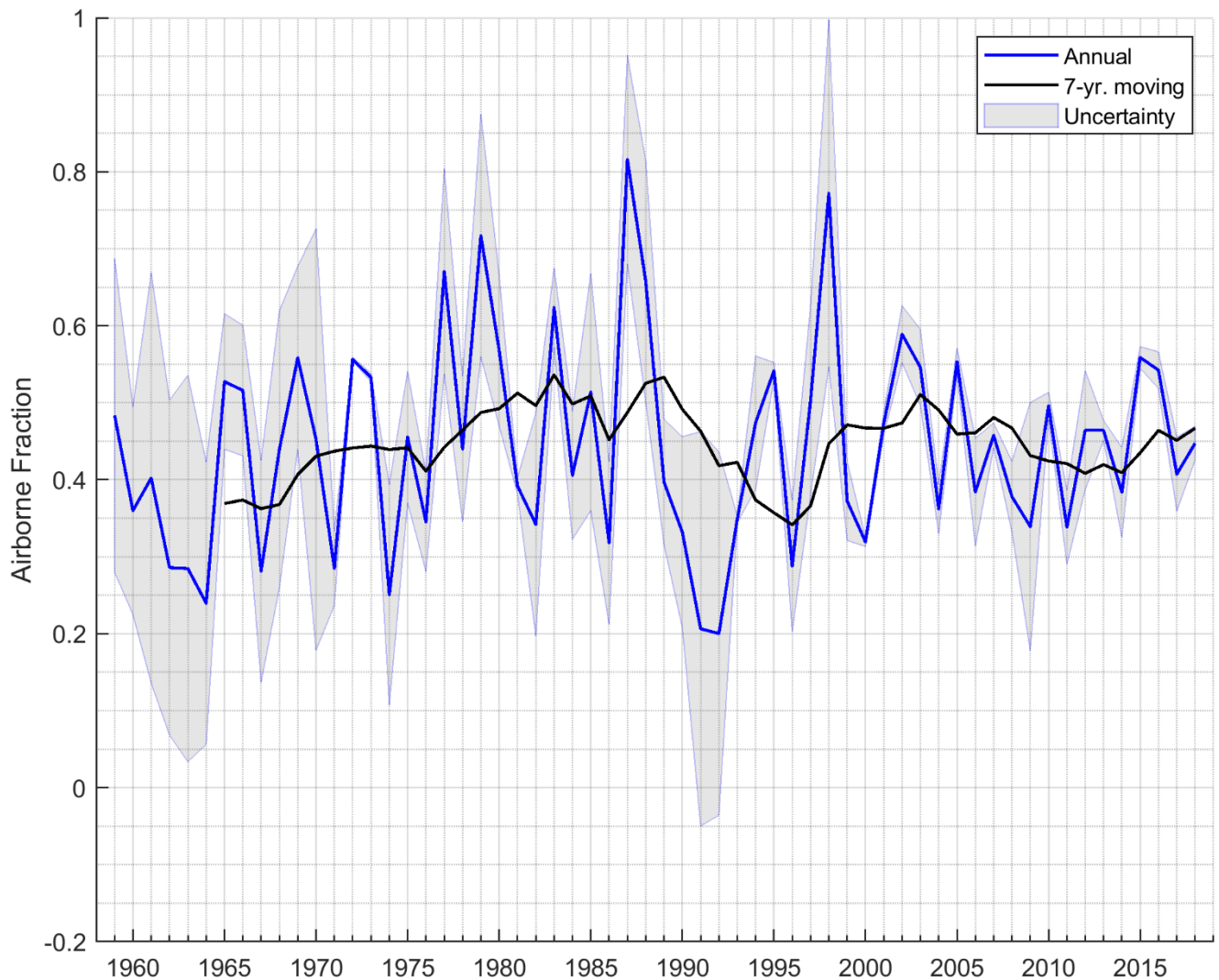
Figure 1. 1959-2018 airborne fraction (*AF*), defined here as the growth in atmospheric CO₂ – or the atmospheric CO₂ remaining after removals by ocean and terrestrial sinks – relative to anthropogenic CO₂ emissions (fossil fuels and LULCC). "Uncertainty" is defined as *AF* ± |*BI*|/*E*, where *E* are total anthropogenic CO₂ emissions and *BI* is the budget imbalance – or *E* minus the sum of atmospheric CO₂ growth and CO₂ sinks. Underlying data are from the Global Carbon Project (Friedlingstein et al., 2019).

190

More importantly, use of AF in Eq. (6) means that time-dependent atmospheric CO_2 removal processes following emissions are not explicitly represented. However, using the AF may be justifiable in some contexts – such as when $\Delta\alpha$ has no time dependency (on inter-annual scales). For example, the pioneering study by Betts (2000) – to which almost all CO_2-eq. literature for $\Delta\alpha$ may be traced (Table 1) – made use of AF when estimating CO_2-equivalence of $RF_{\Delta\alpha}$ because the research objective

195   was to compare an albedo contrast between a fully grown forest and a cropland (i.e, $\Delta\alpha$) to the stock of CO_2 in the forest – a stock that had been assumed to accumulate over 80 yrs. which is the approximate time frame over which Earth's CO_2 sinks

function to remove atmospheric CO_2 to a level conveniently represented by the chosen AF. Had a transient or interannual $\Delta\alpha$ scenario been modeled, however, applying the *EESF* method at each time step of the scenario would have severely overestimated CO_2-equivalent emissions.

200

For this reason, Bright *et al.* (2016) argued that for time-dependent $\Delta\alpha$ scenarios (i.e., when $\Delta\alpha$ evolves over interannual time scales), the time-dependency of CO_2 removal processes (atmospheric decay) following emissions should be taken explicitly into account when estimating the effect characterized in terms of CO_2-equivalent emissions (or removals), thus proposing an alternate metric termed "time-dependent emissions equivalence" -- or *TDEE*:

205

$$TDEE = A_E^{-1}k_{CO_2}^{-1}Y_{CO_2}^{-1}RF_{\Delta\alpha}^*$$ (7)

where *TDEE* is a column vector of CO_2-equivalent emission (or removal) pulses (i.e., one-offs) with length defined by the number of time steps (e.g., years) included in the $\Delta\alpha$ time series (in kg CO_2-eq. m^{-2} yr^{-1}), $RF_{\Delta\alpha}^*$ is a column vector of the local
210 annual mean instantaneous $RF_{\Delta\alpha}$ (in W m^{-2}) corresponding to the $\Delta\alpha$ time series (or $RF_{\Delta\alpha}(t)$), and Y_{CO_2} is a lower triangular matrix with column (row) elements as the atmospheric CO_2 fraction decreasing (increasing) with time (i.e., $y_{CO_2}(t)$). The elements in vector *TDEE* thus give the CO_2-equivalent series of emission (or removal) pulses in time yielding the instantaneous $RF_{\Delta\alpha}$ time profile ($RF_{\Delta\alpha}(t)$) corresponding to the temporally-explicit $\Delta\alpha$ scenario ($\Delta\alpha(t)$). Summing all elements in *TDEE* (i.e., $\sum TDEE$) gives a measure of the accumulated CO_2-eq. emissions (removals) over time. The *TDEE* approach is
215 conceptually similar to the CO_2-forcing-equivalence ("CO_2-fe") approach (Jenkins et al., 2018;Zickfeld et al., 2009) building on the notion of a "forcing equivalent" index (Wigley, 1998).

Time-dependent metrics like the well-known Global Warming Potential (*GWP*) (Shine et al., 1990;Rogers and Stephens, 1988) have also been applied to characterize $\Delta\alpha(t)$, which accumulates $RF_{\Delta\alpha}(t)$ over time (temporally-discretized) up to some
220 policy or metric time horizon (*TH*) which is then normalized to the temporally-accumulated radiative forcing following a unit pulse CO_2 emission over the same *TH*:

$$GWP_{\Delta\alpha}(TH) = \frac{\sum_0^{t=TH} RF_{\Delta\alpha}(t)}{A_E k_{CO_2} \sum_0^{t=TH} y_{CO_2}(t)}$$ (8)

225 where *TH* is the temporal accumulation or metric time horizon. Because it is a cumulative measure, studies making use of *GWP* often divide by the number of time steps (*TH*) to approximate an annual CO_2 flux (e.g., Carrer et al., (2018)). The result of Eq. (8) can be interpreted an equivalentpulse of CO_2 (in kg CO_2-eq. m^{-2}) at $t = 0$ giving the same time-integrated *RF* at *TH* as that following a 1 kg pulse of CO_2.

3.1 Metric permutations

230 Some studies have applied various permutations of the three metrics presented above. For instance, some have applied definitions of the airborne fraction (AF) based on CO_2's pulse-response function (i.e., $y_{CO_2}(t)$) when estimating *EESF* on the grounds that the analysis required a long and forward-looking time perspective (Caiazzo et al., 2014;Favero et al., 2018;Mykleby et al., 2017;Muñoz et al., 2010;Sciusco et al., 2020). A consequence is that the magnitude of the CO_2-eq. calculation is highly sensitive to the subjective choice of the *TH* chosen as the basis for the AF (typically taken as the mean

235 atmospheric fraction for the period up to TH – or $TH^{-1} \int_{t=0}^{t=TH} y_{CO_2}(t)\, dt$). Other permutations include the normalization of *EESF* or *GWP(TH)* by *TH* to arrive at a uniform time series of CO_2-eq. pulses (Carrer et al., 2018), or the summing of *TDEE* up to *TH* to obtain a CO_2-eq. stock perturbation measure (Bright et al., 2020;Bright et al., 2016).

3.2 Metric decision tree

Their relative merits and drawbacks (further discussed in Sections 4 & 5) notwithstanding, Figure 2 presents a decision tree

240 for differentiating between the reviewed *Δα* metrics presented heretofore.
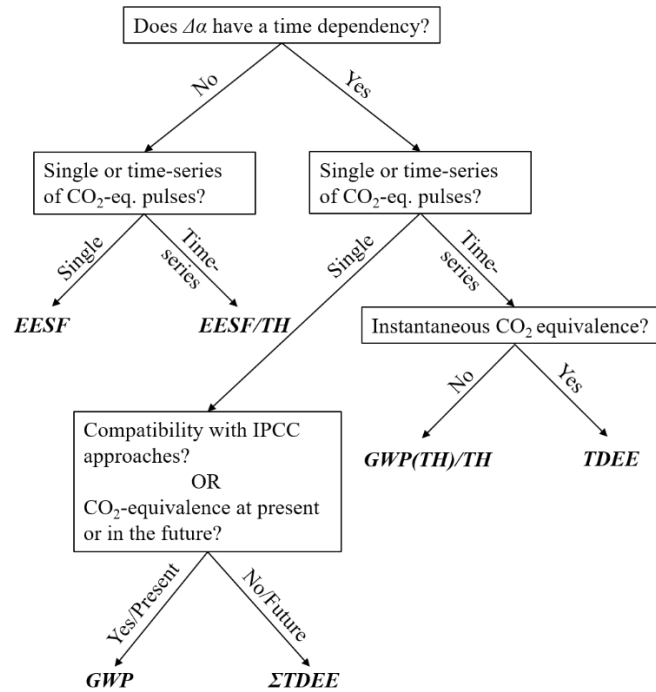
Figure 2. Decision-tree for metrics applied in the literature included in this review to assess *Δα*.

245 A principle differentiator after the time-dependency distinction is whether CO_2-equivalence corresponds to a single emission (removal) pulse or a time series of multiple CO_2-equivalent emission (removal) pulses. For the time-dependent metrics (Fig. 2, right branch), further distinction can be made according to whether the CO_2-equivalent effect is an instantaneous effect (in the case of the time-series measures) and whether IPCC compatibility is desired by the practitioner (in the case of the single pulse measures). By "IPCC compatibility", we mean that the metric computation and physical interpretation aligns with

250 emission metrics presented in previous IPCC climate assessment reports and IPCC good practice guidelines for national emission inventory reporting. A second or alternate distinction can be made for the time-dependent and single pulse measures according to whether the CO_2-equivalent effect corresponds to the present ($t = 0$) or the future ($t = TH$).

3.3 Δα vs. emission metrics

All metric application entails subjective user decisions, such as type of metric (i.e., instantaneous vs. accumulative; scalar vs.

255 time-series) and time horizon for impact evaluation. CO_2-eq. metrics for $\Delta\alpha$ require additional decisions by the practitioner affecting both their transparency and uncertainty, which are highlighted in Table 3.

Table 3. Important decisions required by the practitioner to obtain a CO_2-eq. metric for $\Delta\alpha$ (based on RF) relative to conventional CO_2-normalized emission metrics of the IPCC (i.e., GWP).

Radiative forcing agent	*RF* Metric	Initial Perturbation (emission or $\Delta\alpha$)	Perturbation time-dependency	*RF* model
GHGs	*GWP*	Unit pulse	IPCC	IPCC
$\Delta\alpha$, time-dependent	*TDEE; GWP*	User defined	User-defined	User defined
$\Delta\alpha$, time-independent	*EESF*	User defined	None	User defined

260

First among these is the need to quantify the initial physical perturbation (i.e., $\Delta\alpha$) which is irrelevant for IPCC emission metrics where the initial perturbation is a unit pulse emission. For $\Delta\alpha$ metrics, uncertainty surrounding estimates of the initial (or reference) and perturbed albedo states is introduced. Second, for the time-dependent metrics (Table 3, second row)

265 additional uncertainty is introduced by the metric practitioner when defining the time-dependency of the $\Delta\alpha$ perturbation, which may be contrasted to IPCC emission metrics where the temporal evolution of the perturbation (i.e., atmospheric concentration change) is pre-defined (or rather, lifetimes and decay functions of the various forcing agents). Likewise, the *RF* models employed to give radiative efficiencies for various forcing agents are pre-defined by the IPCC -- models having origins linked to standardized experiments employing rigorously evaluated radiative transfer and/or climate models, which may be

270   contrasted to the models applied to estimate $RF_{\Delta\alpha}$ which can vary widely in their complexity and uncertainty (for a brief review of these, see Bright & O'Halloran (2019)).

4 Quantitative metric evaluation

The metrics presented in Section 3 are systematically compared quantitatively henceforth by deriving them for a set of common cases, starting first with the metrics applied to yield a time series of CO_2-eq. pulse emissions (or removals) in time. For all

275   calculations, the assumed climate "efficacy" (Hansen et al., 2005) – or the global climate sensitivity of $RF_{\Delta\alpha}$ relative to RF_{CO_2}

    – is 1.

4.1 CO₂-eq. pulse time series measures

Let us first consider a geoengineering case where one m^2 of a rooftop is painted white during the first year of a 100-year simulation which increases the annual mean surface albedo (Fig. 3 A) for the full simulation period resulting in a constant

280   negative $RF_{\Delta\alpha}$ (Fig. 3 B). The objective is to estimate a series of CO_2-eq. fluxes associated with the local $RF_{\Delta\alpha}(t)$.
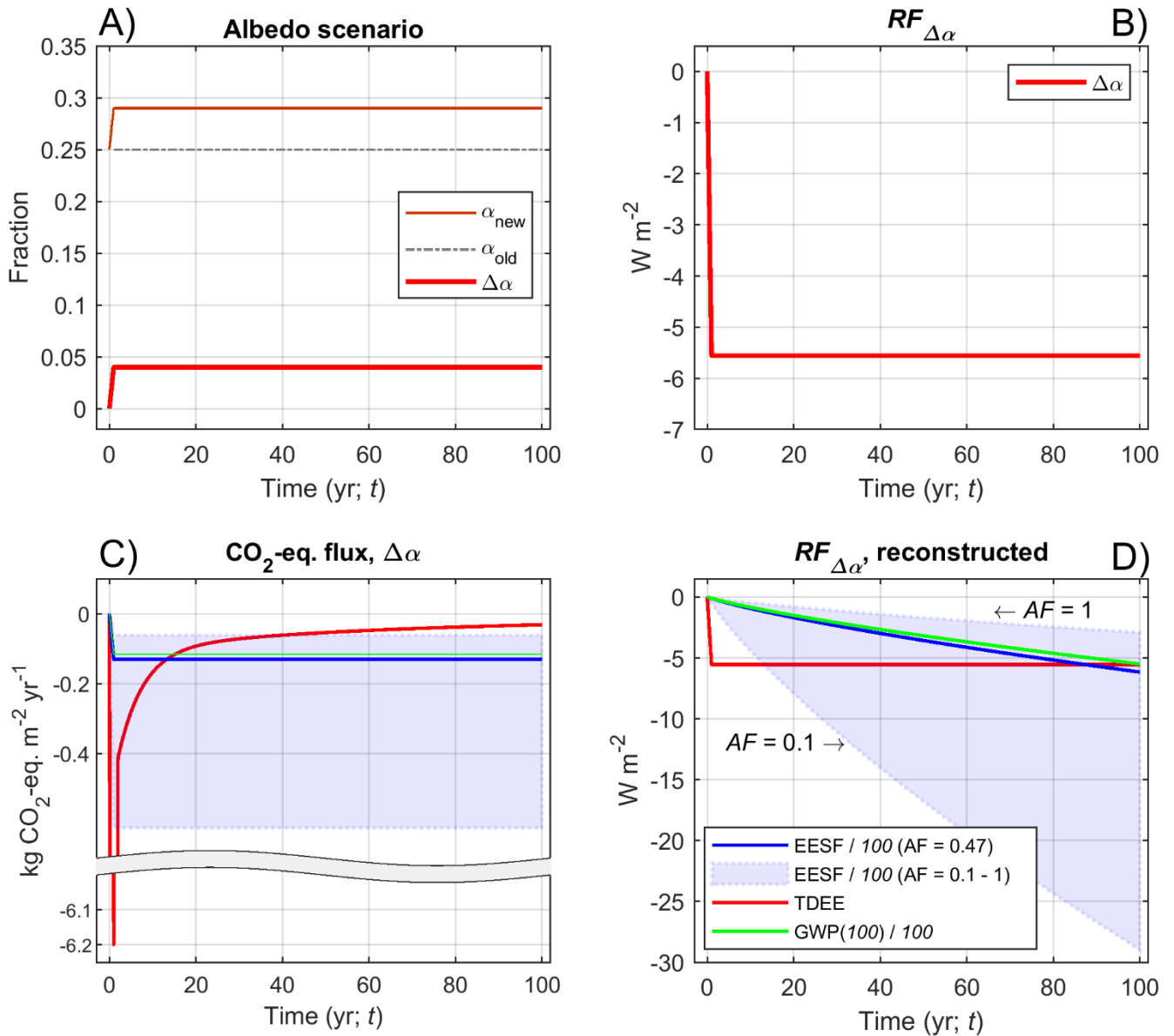
Figure 3. Example application of metrics yielding a complete time series of CO_2-eq. pulse emissions or removals. A) Time-dependent local $\Delta\alpha$ scenario ("$\Delta\alpha$" = α_{new} - α_{old}); **B)** The corresponding local annual mean instantaneous shortwave radiative forcing over time ($RF_{\Delta\alpha}(t)$); **C)** The derived metrics *TDEE*, *GWP(100)/100*, and *EESF/100* for a range of airborne fractions (AF), ; **D)** The reconstructed local annual mean $RF_{\Delta\alpha}(t)$ based on the values shown in panel C) and Eq. **(4)**. Note that the legend in panel D) also applies to panel C).

Figure 3 C presents the results after applying the relevant metrics to the common $RF_{\Delta\alpha}$ and time-dependent $\Delta\alpha$ scenario. To assess their fidelity or "accuracy", the resulting CO_2-eq. series of annual CO_2 pulses (in this case removals) are used with Eq. (4) to re-construct the $RF_{\Delta\alpha}$ time profile (Fig. 3 B). Unsurprisingly, annual CO_2-eq. removals estimated with the *TDEE*

approach (Fig. 3 C) exactly reproduce $RF_{\Delta\alpha}$, and thus the two red curves shown in Figures 2B and D are identical (note the difference in scale). Figure 3 C illustrates the sensitivity of the *EESF*-based measure derived using an AF of 0.47 (mean of the last seven years based on the most recent global carbon budget, e.g. Friedlingstein et al., 2019; Fig. 1) relative to a broad range of AF values (note that the result obtained using AF = 1 is referred to as the "time-independent emissions equivalent (*TIEE*)" presented in Bright et al. (2016)). Irrespective of the AF value that is chosen, when applied in a forward-looking analysis utilizing a time-dependent $\Delta\alpha$ scenario with a time horizon of 100-yrs., the *EESF* approach underestimates the magnitude of the annual CO_2-eq. pulse occurring in the short-term relative to *TDEE* (Fig. 3 C) and hence also $RF_{\Delta\alpha}$ in the short-term (Fig. 3 B & D). This is because the CO_2 forcing represented as $TH^{-1}k_{CO2}AF$ with the *EESF* approach is weaker than the CO_2 forcing represented as $k_{CO2}\sum_{t=0}^{t=TH} y_{CO_2}(t)$ with the *TDEE* approach in the short-term. For higher AF values, annual CO_2-eq. removals estimated using the *EESF*-based approach will underestimate the $RF_{\Delta\alpha}$ at each time step (Fig. 3 D), despite the higher magnitude CO_2-eq. estimate (relative to *TDEE*) seen in the longer-term (Fig. 3 C). This is owed to the lower atmospheric CO_2-equivalent abundance that is accumulated over the period when the series of annual CO_2-eq. fluxes are reduced to compensate for the higher *AF*.

For *TH* = 100 years, the *EESF*-based estimate will always be lower in magnitude in the short-term and higher in magnitude in the longer-term relative to *TDEE* (Fig. 3 C). The same is also true for the annual *GWP*-based CO_2-eq. estimate, although at least the reconstructed $RF_{\Delta\alpha}$ value at $t = TH$ will always be identical to the actual $RF_{\Delta\alpha}$ value at $t = TH$ (Fig. 3 D). In general, *EESF*- and *GWP*-based estimates of annualized CO_2-eq. emissions (or removals) are sensitive to the chosen *TH* and will always exceed (in magnitude) estimates based on *TDEE*. This is demonstrated in Figure 4.
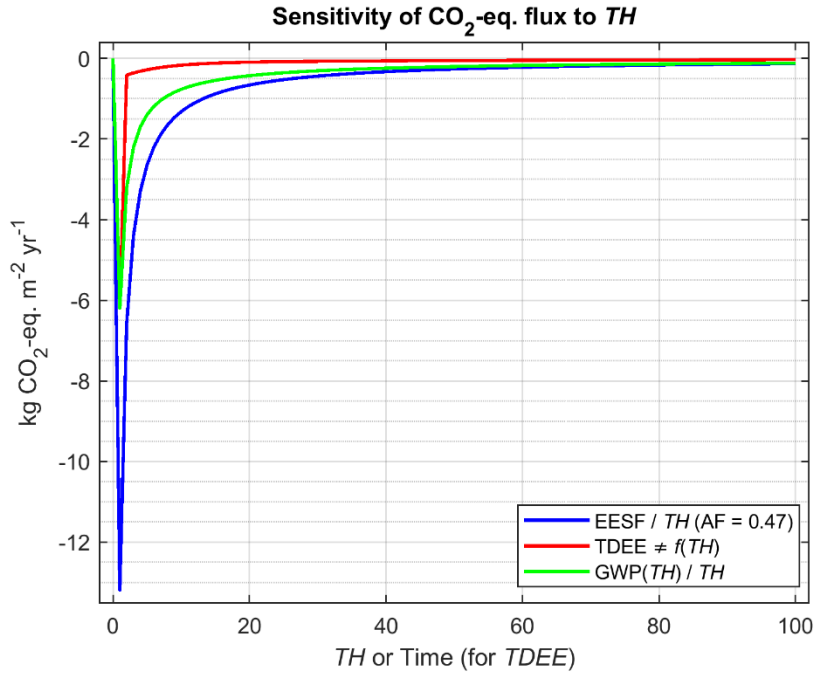
Figure 4. Magnitude of the annual CO2-eq. emission (removal) pulse as a function of metric *TH* for the *EESF* and *GWP* measures relative to *TDEE* which is insensitive to *TH*.

The *EESF*-based estimate in this example is higher (in magnitude) than the GWP-based estimate because the assumed AF of 0.47 is lower than the mean atmospheric fraction following pulse emissions (i.e., $y_{CO_2}(t)$) over the range of time horizons shown (the mean atmospheric fraction at $TH = 100$ when applying Joos et al. (2013) function is 0.53). In contrast to the *EESF*- and *GWP*-based approaches, the magnitude of the annual CO_2-eq. removals estimated with *TDEE* is insensitive to the chosen *TH*.

4.2 Single CO2-eq. pulse measures

Turning our attention now to measures yielding a single CO_2-eq. emission or removal pulse, let us now consider a forest management case where managers are considering harvesting a deciduous broadleaf forest to plant a more productive evergreen needleleaved tree species. It is known that when the evergreen needleleaf forest matures in 80-years its mean annual surface albedo will be about 2% lower than the deciduous broadleaved forest. The corresponding annual local $RF_{\Delta\alpha}$ at year 80 is 1.8 W m^{-2}, and we wish to associate a CO_2-equivalence to this value in order to weigh it against an estimate of the total CO_2 stock difference between the two forests after 80 years (i.e., $TH = 80$). Assuming we have no information about how the albedo evolves *a priori* in the two forests before year 80, we have no choice but to apply the *EESF* measure.

Figure 5 presents the CO_2-eq. estimate based on *EESF* for an AF range of $0.1 - 1$, shown together with an estimate in which the AF is obtained using the mean fraction of CO_2 remaining in the atmosphere at 80 years following an emission pulse, obtained from the latest IPCC impulse-response function ($y_{CO_2}(t)$), and with the highest and lowest airborne fractions of the last 7 years.
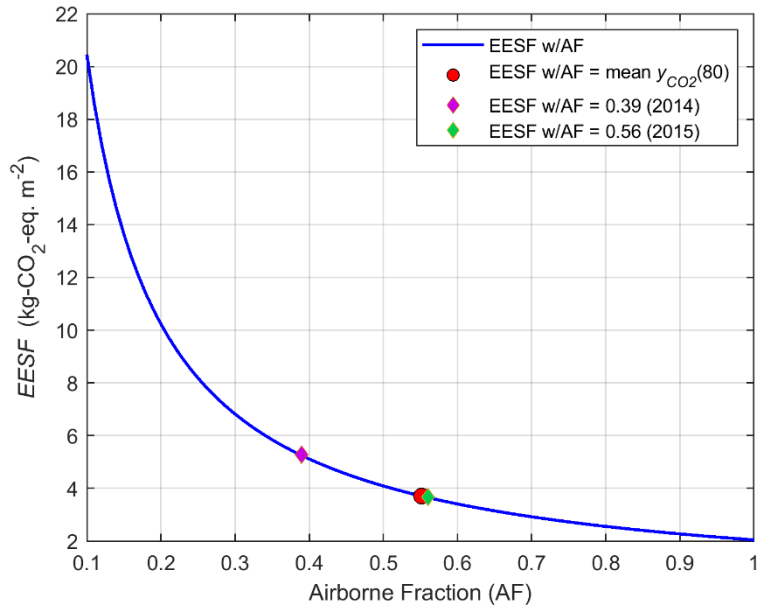
Figure 5. Sensitivity of *EESF* to the airborne fraction (AF).

Figure 5 illustrates *EESF*'s sensitivity to the assumed AF. For instance, *EESF* with AF = 0.3 is double that estimated with AF = 0.6 – a normal AF range for the past 60 years (Fig. 1). *EESF* estimated using AF from 2015 (Fig. 5, green diamond) is 44% lower than *EESF* using AF from the previous year (Fig. 5, magenta diamond). If surface albedo is ever to be included in forestry decision-making – as some have proposed (Thompson et al., 2009a;Lutz and Howarth, 2014) – the subjective choice of the AF becomes problematic given this large sensitivity. For instance, if the decision-making basis in this example depends on the net of the CO_2-eq. of $\Delta\alpha$ and a difference in forest CO_2 stock of 4.5 kg CO_2 m^{-2}, adopting an AF of 0.5 might lead to a decision to plant the new tree species given that the stock difference would exceed the *EESF* estimate (i.e., CO_2 sinks dominate), whereas adopting an AF of 0.4 might lead to a decision to forego the planting given that the CO_2-eq. of $\Delta\alpha$ would exceed the stock difference (i.e., surface albedo dominates).

Now let's assume the metric user *does* have insight into how the surface albedos of both forest types will evolve over the full rotation period. In this new example, harvesting the deciduous broadleaf forest to plant an evergreen needleleaf species will first increase the surface albedo in the short-term, yet as the evergreen needleleaf forest grows and tree canopies begin to close and mask the surface, the albedo difference ($\Delta\alpha$) reverts to negative and stays negative for the remainder of the rotation. This

results in an annual mean local $RF_{\Delta\alpha}(t)$ profile that is first negative and then positive, which is depicted in Figure 6 A (blue solid curve, left y-axis).

355
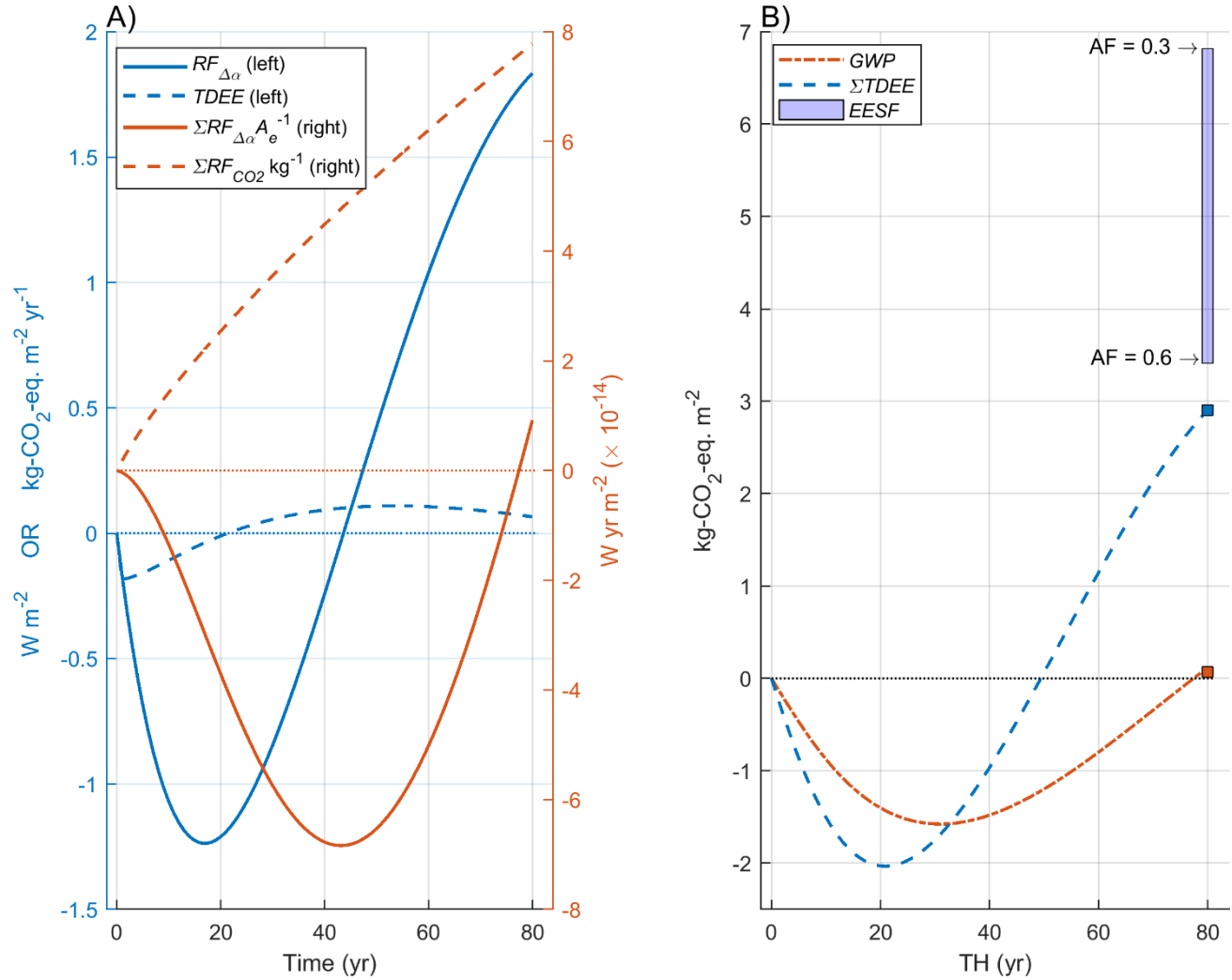
Figure 6. Example application of metrics yielding a single CO₂-eq. emission (or removal) pulse following a hypothetical forest tree species conversion. A) $RF_{\Delta\alpha}(t)$ **and corresponding** *TDEE* **(left y-axis, blue curves) and the temporally-accumulated** $RF_{\Delta\alpha}(t)$ **normalized to Earth's surface area (solid red, right y-axis) and temporally-accumulated** $RF_{CO_2}(t)$ **(dashed red, right y-axis) following a 1 kg pulse emission ; B)** *EESF* **estimated for the** $\Delta\alpha$ **(and** $RF_{\Delta\alpha}$**) occurring at** *TH* **= 80 shown in relation to** *GWP(TH)* **–**
360 **or the ratio of two red curves shown in panel A – and** $\sum TDEE$ **estimated at all** *THs.*

Converting the $RF_{\Delta\alpha}(t)$ time profile first to a time series of CO₂-eq. emission/removal pulses (i.e., *TDEE*, Fig. 6 A, dashed blue curve) then summing to year 80 gives a measure of the total quantity of CO₂-eq. emitted (or removed) at year 80 – or $\sum TDEE$ (Fig. 6 B, blue curve). $\sum TDEE$ thus "remembers" the negative $\Delta\alpha$ in the early phases of the rotation period (short-
365 term), leading to a lower CO₂-eq. estimate at year 80 relative to *EESF* estimates computed with airborne fractions of 0.66 and

lower. Similarly, the *GWP*-based estimate "remembers" the negative $\Delta\alpha$ occurring in the short-term; however, *GWP* is a normalized measure, meaning that the time-evolving radiative effects of $\Delta\alpha$ and CO_2 are first computed independently from each other prior to the CO_2-equivalence calculation, whereas for *TDEE* (and hence $\sum TDEE$) CO_2-equivalence depends *directly* on the time-evolving radiative effect of $\Delta\alpha$. Framed differently, $\sum TDEE$ remembers prior CO_2-eq. fluxes yielding the

370 radiatively equivalent effect of the time-dependent $\Delta\alpha$ scenario, whereas the "memories" of $RF_{\Delta\alpha}$ and RF_{CO2} underlying the *GWP*-based CO_2-equivalent estimate are first considered in isolation (Fig. 6 A, red curves). Hence the *GWP*-based CO_2-eq. estimate in this example is much lower than the $\sum TDEE$-based estimate since the temporally-accumulated RF_{CO2} following a unit pulse emission at $t = 0$ (or ΣRF_{CO2}, also known as the Absolute GWP or $AGWP_{CO2}$, Fig. 6A dashed red curve) is significantly larger than the temporally-accumulated $RF_{\Delta\alpha}$ (or $\Sigma RF_{\Delta\alpha}$) representing brief periods of both positive- and negative

375 $RF_{\Delta\alpha}$. Comparing brief or "short-lived" *RF*s with CO_2 *RF*s using *GWP* has been heavily criticized for reasons we discuss further in Section 6.

When scalar metrics are required, Figure 6 illustrates the large inherent risk of applying a static measure like *EESF* to characterize $\Delta\alpha$ in dynamic systems. Moreover, for dynamic systems in which $\Delta\alpha$'s time-dependency is defined *a priori*, Fig. 6 illustrates the importance of clearly defining the time horizon at which the physical effects of $\Delta\alpha$ and CO_2 are to be compared:

380 *GWP* gives an effect measured in terms of a present-day CO_2 emission (or removal) pulse, while $\sum TDEE$ gives an effect measured in terms of a future CO_2 emission (or removal). In other words, internal consistency between the ecological and metric time horizons is relaxed with *GWP* but preserved with $\sum TDEE$.

5 Qualitative metric evaluation

The reviewed metrics and underlying methods for converting shortwave radiative forcings from $\Delta\alpha$ (i.e., $RF_{\Delta\alpha}$) into their CO_2

385 equivalent effects – summarized in Table 4 – can primarily be differentiated by the physical interpretation of the derived measure and by whether or not a time-dependency (inter-annual) for $\Delta\alpha$ was defined *a priori*.

Table 4. Overview of distinguishing attributes, methodological differences, drawbacks, and merits of the six $\Delta\alpha$ metrics applied in the scientific literature included in this review.

$\Delta\alpha$ Metric	CO_2-equivalence Interpretation	Time-dependent $\Delta\alpha$ scenario	Drawbacks		Merits	
EESF	Single pulse	No	-	Sensitive to choice of airborne fraction (AF)	-	Easy to apply; No need to define a $\Delta\alpha$ scenario *a priori*
			-	Not forward-looking		
			-	No carbon cycle dynamics		

EESF/TH	Series of uniform pulses	No	- Same as above - CO_2-eq. series does not reproduce $RF_{\Delta\alpha}(t)$ [a] - Sensitive to *TH*	- Easy to apply
TDEE	Series of non-uniform pulses	Yes	- Not scalar	- CO_2-eq. series reproduces $RF_{\Delta\alpha}(t)$ - Can be compared to an emission scenario - Insensitive to *TH*
ΣTDEE	Accumulation of a series of non-uniform pulses	Yes	- Cannot be compared to a CO_2 pulse of the present	- Compatible with policy targets based on cumulative emissions - Insensitive to *TH*
GWP	Single pulse	Yes	- Sensitive to *TH* - May be a poor indicator of impact when $\Delta\alpha(t)$ is shorter than *TH*.	- Well-known; IPCC conformity - Compatible with IPCC assessments and UNFCCC accounting conventions
GWP(TH) /TH	Series of uniform pulses	Yes	- Sensitive to *TH* - CO_2-eq. series does not reproduce $RF_{\Delta\alpha}(t)$ except at $t = TH$	- *GWP* method is well-known

390 [a] The exception is at $t = TH$ when $AF = TH^{-1} \int_{t=0}^{t=TH} y_{CO_2}(t)\, dt$

For cases when $\Delta\alpha$'s time-dependency is not known or defined *a priori*, the *EESF* measure is the only applicable measure of those reviewed, although it was shown here to be highly sensitive to the value chosen to represent CO_2's airborne fraction (AF; Fig. 5) – a key input variable taking on a wide range of values depending on how it was defined. In general, when AF is

395 defined according to historical accounts of global carbon cycling, its value is prone to large fluctuations across short time scales (Fig. 1) due to natural variability in the global carbon cycle (Ciais et al., 2013). When defined as the fraction of CO_2 remaining in the atmosphere following a pulse emission – as would be obtained from a simple carbon cycle model (i.e., a CO_2 impulse-response function) -- its value depends on the time horizon chosen and underlying model representation of atmospheric removal processes (i.e., time-constants). Use of the latter definition of AF affixes a forward-looking time-

400 dependency to the *EESF* measure which is inconsistent with the definition of $\Delta\alpha$ and adds subjectivity (i.e., the choice in *TH*). Basing the AF on global carbon budget reconstructions would at least preserve some element of objectivity, although given

the measure's sensitivity to AF it would be prudent to compute the measure for a range of AFs (i.e., as constrained by the observational record) in effort to boost transparency. Forgoing the use of an AF altogether would eliminate all subjectivity, as has been suggested elsewhere (Bright et al., 2016).

405

For cases involving a time-dependent $\Delta\alpha$ scenario that is defined *a priori*, forward-looking measures are identified whose methodological differences give rise to different interpretations of "CO_2-equivalence" (Table 4). For example, the *GWP* measure can be interpreted as CO_2-eq. pulse emitted at present yielding the accumulated radiative forcing of the $\Delta\alpha$ scenario at *TH* years into the future. *GWP* has merit from the standpoint that it is easy to apply and conforms to established reporting

410 methods, accounting standards, or decision-support tools such as Life Cycle Assessment (e.g., Cherubini et al. (2012); Sieber et al. (2020)). Scientifically, however, there are important limitations to *GWP* when the forcing (i.e., $\Delta\alpha$) is short-lived or temporary (Allen et al., 2016;Pierrehumbert, 2014;Allen et al., 2018;Lynch et al., 2020;Cain et al., 2019). The *TDEE* measure, on the other hand, can be interpreted as a complete time series of CO_2 emission pulses (i.e., a complete emission scenario) yielding the instantaneous radiative forcing of the $\Delta\alpha$ scenario. When summed to *TH*, the latter (as $\Sigma TDEE$) provides a clearer

415 indication of the radiative impact incurred up to *TH*, thus having greater scientific merit as an indicator of future warming.

The permutations of *GWP* and *EESF* applied to arrive at a time series of CO_2-eq. pulses -- *GWP(TH)/TH* and *EESF/TH* -- have little merit on the grounds that the resulting series does not reproduce $RF_{\Delta\alpha}(t)$ (Fig. 3 D). The *TDEE* approach was proposed to overcome this limitation, although it should be stressed that – like *GWP(TH)/TH* – its derivation requires that a time-

420 dependent $\Delta\alpha$ scenario be defined *a priori*, which adds uncertainty and may not always be possible.

6 *GWP** and $\Delta\alpha$

It has been known that the conventional usage of *GWP* does not adequately capture different behaviors of short-and long-lived climate pollutants or their impact on global mean surface temperatures (Pierrehumbert, 2014;Allen et al., 2016;Shine et al., 2003;Fuglestvedt et al., 2010). Some have proposed an alternative usage of *GWP* – denoted *GWP** (Allen et al., 2018) --

425 which overcomes this problem by equating an increase in the emission rate of a short-lived climate pollutant (or radiative forcing agent) with a one-off "pulse" CO_2 emission. *GWP** recognizes that a pulse emission of CO_2 and a sudden step-change in the sustained rate of emission of a short-lived climate pollutant (SLCP) both give near-constant radiative forcing. Or, alternately, that a progressive linear increase (or decrease) in the rate of an SLCP emission is approximately equivalent to a sustained step change in the emission rate of CO_2. As such, *GWP** is considered to have greater "environmental integrity"

430 than the conventional *GWP* metric (Allen et al., 2018), as it is better fit to serve the purpose of a measure of progress towards a global temperature-oriented climate goal (i.e., limit warming to "well below 2°C"). Compared to conventional *GWP*, cumulative CO_2-eq. emissions based on *GWP** provide a clearer indication of future warming, and future CO_2-eq. emission rates better-indicate future warming rates. *GWP** thus better-relates all climate pollutants in a common cumulative emission

(or emission budget) framework, making it easier to formulate mitigation strategies that provide a more accurate indication of progress towards climate stabilization.

Among one of the more distinguishing features of *GWP** is that, when applied to radiative forcings rather than pulse emissions, information about the time-dependency of the perturbation (i.e., the lifetimes of "climate pollutants" or forcing agents) is not required (Lee et al., 2021;Cain et al., 2019;Allen et al., 2018), making it an attractive alternative to *EESF*. In other words, a *GWP* estimate of the "short-lived" forcing agent under scope – which requires such information to be known or defined *a priori* -- is unnecessary in its calculation. Only the rate of change of the forcing is required, scaled by *TH/AGWP(TH)$_{CO2}$* as follows (Lee et al., 2021;Allen et al., 2018):

$$E_{CO2-eq.*} = \frac{TH}{AGWP(TH)_{CO2}} \left(\frac{\Delta RF_{\Delta\alpha}}{\Delta t} \right) \tag{9}$$

where *TH* is the time horizon, *AGWP(TH)$_{CO2}$* is CO_2's AGWP at the same *TH* (i.e., 9.2×10^{-14} W m^{-2} kg^{-1} year when *TH* = 100 yrs.), Δt is the time step change, and $\Delta RF_{\Delta\alpha}$ is the time-differential of $RF_{\Delta\alpha}(t)$ over the step change. $E_{CO2-eq.*}$ thus represents the CO_2-eq. emission pulse for the step change and will equal *EESF* when the AF (in Eq. 6 denominator) corresponds to the mean of $y_{CO_2}(t)$ over the *TH* (i.e., $TH^{-1} \int_{t=0}^{t=TH} y_{CO_2}(t)\, dt$). A *TH* of 100 years is typically applied in Eq. (9) which is justified when it exceeds the lifetime of the SLCP or when the time-integrated radiative forcing of the forcing agent (i.e, $\Delta\alpha$) becomes a constant at this time scale, since the time-integrated radiative forcing of the reference gas (i.e., $AGWP_{CO2}$) increases linearly with *TH*. In other words, the *TH*-dependence cancels out in the calculation of CO_2-eq.*, rendering *GWP** insensitive to the choice in *TH* which contrasts with the conventional *GWP* (Allen et al., 2016; Allen et al., 2018). The step change Δt for which ΔRF is calculated is typically taken as 20 years to "reduce the volatility of CO_2-eq.* emissions in response to variations in SLCP emission rates" (Allen et al. 2018; Cain et al. 2019), although comprehensive investigations into the appropriateness of this choice when applied to a wide variety of time-varying SLCP emission (radiative forcing) scenarios are lacking. We note that more recent works (Cain et al., 2019; Lee et al., 2020) employed weighting-based modifications to Eq. (9) in effort to better-account for the longer-term temperature equilibration to past forcing changes. Like the choice of Δt, however, few investigations into the appropriateness of weight sizes employed in the modified *GWP** expression (not presented; see Eqs. (1) in Cain et al., 2019 and Lee et al., 2020) for a wide variety of time-varying SLCP (radiative forcing) scenarios have been carried out.

We explore the sensitivity of the choice in both Δt and the "stock contribution" weighting factor (referred to as "*s*" in Cain et al., 2019 and "α" in Lee et al., 2020) on CO_2-eq. emissions (removals) estimated with the *GWP** approach -- or Eq. (1) in Lee et al. (2020) – for three hypothetical local $RF_{\Delta\alpha}(t)$ scenarios presented in Figure 7 A, the first of which ("Scenario A") being

identical to the forest management scenario plotted in Figure 6 A and extended by 20-yrs, which is characterized by a negative *RF* in short-term and positive *RF* in the longer-term (Fig. 7 A, blue). $RF_{\Delta\alpha}(t)$ in Scenario B corresponds to a linearly increasing $\Delta\alpha$ trend which is loosely analogous to incremental deforestation occurring on a regional scale (Fig. 7 A, red), and Scenario C resembles a permanent albedo decrease, analogous to urban expansion into a cropland (Fig. 7 A, yellow).

470
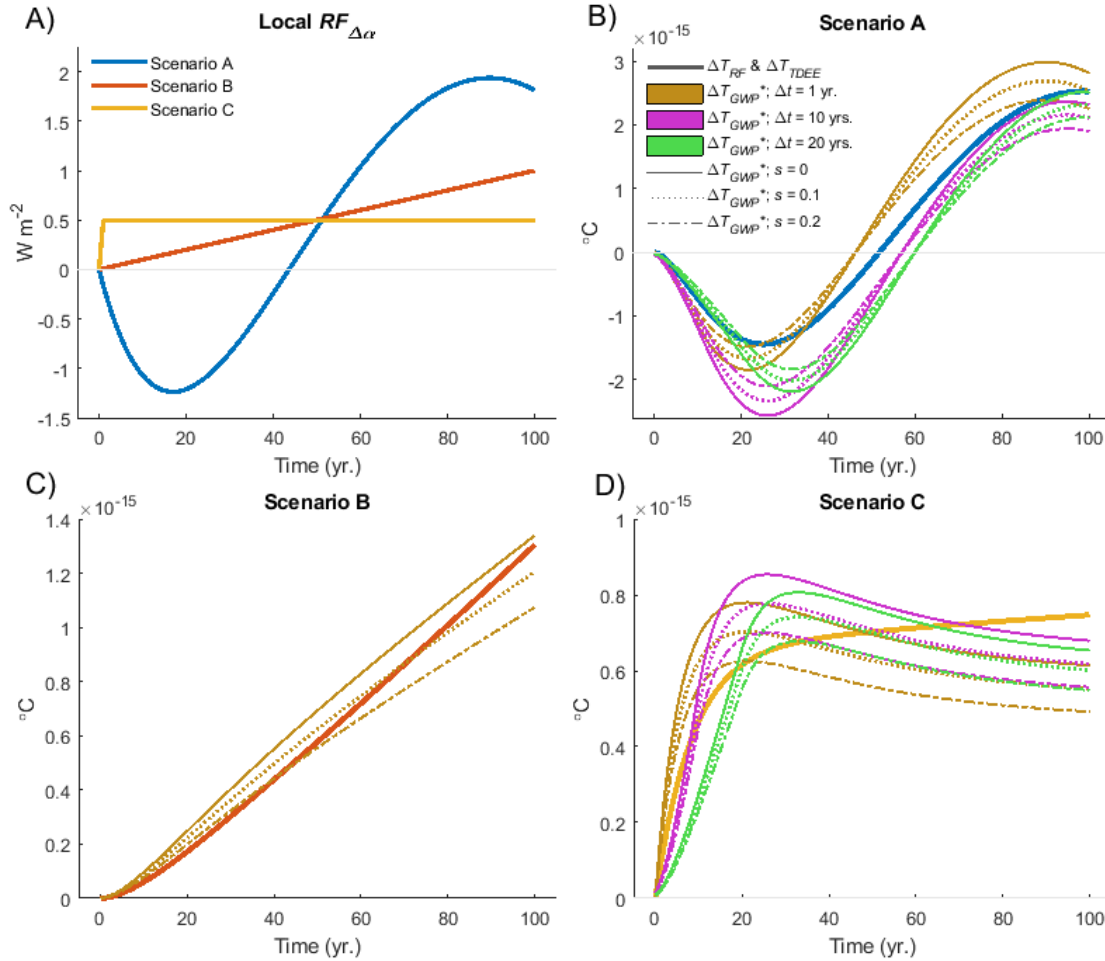
Figure 7. Performance of *GWP** computed with nine different parameter sets for three stylized scenarios of surface albedo change-driven radiative forcing. A) Local radiative forcing of one permanent and two temporally-evolving surface albedo change scenarios; B-D) The corresponding global mean temperature response ΔT to the radiative forcing relative to that which has been reconstructed using the CO_2-eq. emission (removal) time series computed with *TDEE* and *GWP** under the assumption that $\Delta\alpha_{t+n-t}$ is known. ΔT in panels B-D is estimated with a temperature impulse response function following (Boucher and Reddy, 2008;Myhre et al., 2013) having a climate sensitivity of 1.06 K (W m^{-2})$^{-1}$, which is equivalent to a 3.9 K equilibrium climate response to an abrupt CO_2 concentration doubling.

480

We then reconstruct the global mean temperature response (ΔT) of the CO_2-eq.* emission (removal) scenario under varying assumptions surrounding the size of Δt and the "stock contribution" weighting factor s, which is then compared to the $RF_{\Delta\alpha}$-based ΔT and the ΔT reconstructed using the CO_2-eq. emission (removal) scenario based on the *TDEE* approach (Fig. 7 B-D). For Scenario A (Fig. 7 B), we find no obvious parameter set that outperforms any other in terms of the faithfulness by which

485   the CO_2-eq* emission (removal) scenario reproduces ΔT across the full time horizon. There appears to be a trade-off between the near- and long-term reproduction accuracy of different parameter sets: a 20-yr Δt with no weighting (Fig. 7 B, solid green curve) better-reproduces the ΔT response seen in the short-term ($\sim$ <20 yrs.) as well as the ΔT seen at the end of the scenario time horizon (year 100), whereas a 10-yr Δt with no weighting (Fig. 7 B, solid purple curve) better-reproduces the ΔT response seen in the longer-term (from ~60-90 yrs.). An increase to the weighting factor s serves to dampen the amplitude between the

490   maximum cooling and warming seen in the short- and longer-terms, respectively (Fig. 7 B, spread between like-colored curves). As for Scenario B representing a linear increase in RF, the reconstructed ΔT is insensitive to Δt and thus only results for a 1-year Δt are computed and presented in Figure 7 C. Although a weighting factor of 0.2 is most accurate for the first ~50 years, a weight of 0.1 gives a more faithful ΔT reproduction for the full time period. As for Scenario C representing a step change in RF (Fig. 7 D), again we find no obvious parameter set that yields a faithful ΔT reproduction across the full time

495   period. High s weights overpredict ΔT in the medium-term but reproduce ΔT best in the longer-term (Fig. 7 D, solid curves), while a Δt larger than 10 years appears to result in large underpredictions in the short-term (i.e., < ~ 20 yrs; Fig. 7 D, green curves).

Unsurprisingly, ΔT reconstructed using the CO_2-eq. emission (removal) scenario estimated with the *TDEE* approach exactly

500   reproduces the RF-based ΔT and thus these two estimates are plotted jointly as a single curve in Figure 7 B-D (wider solid curves). Thus, when future surface albedo changes are defined *a priori* (i.e., when the $\Delta\alpha$ perturbation "lifetime" is known or estimated), a CO_2-eq. emission (removal) time series quantified with *TDEE* is far superior to one based on *GWP** irrespective of the choice in Δt or weight sizes applied, making it the better CO_2-eq. measure of progress towards global temperature stabilization.

505   **7 Spatial disparity in climate response between CO_2 emissions and $\Delta\alpha$ perturbations**

The climate (i.e., temperature) response to a $\Delta\alpha$ perturbation either isolated (e.g., Jacobson and Ten Hoeve, (2012)) or as part of LULCC (e.g., (Pongratz et al., 2010;Betts, 2001)) is highly heterogeneous in space, the magnitude and extent of which depends on its location (Brovkin et al., 2013;de Noblet-Ducoudré et al., 2012). This is because the response pattern of climate feedbacks has a strong spatial dependency – feedbacks are generally larger at higher latitudes due to higher energy budget

510   sensitivity to clouds, water vapor, and surface albedo, which generally increases the effectiveness of RF in those regions (Shindell et al., 2015). This is in contrast to CO_2 emissions where both RF and the temperature response are more homogeneous

in space (Hansen and Nazarenko, 2004;Hansen et al., 2005;Myhre et al., 2013). This has caused some researchers to question the utility of a CO2-eq. measure for $\Delta\alpha$ (Jones et al., 2013) or encouraged others to look for solutions or further methodological refinements. For instance, some researchers (e.g., Cherubini et al. (2012); Zhao & Jackson (2014)) have applied climate

515   "efficacies" – or the climate sensitivity of a forcing agent relative to CO2 (Joshi et al., 2003;Hansen et al., 2005) – to adjust $RF_{\Delta\alpha}$ prior to the CO2-eq. calculation. Such adjustments recognize that the temperature response to RF depends on the geographic location, extent, and type of underlying forcing associated with the $\Delta\alpha$ (e.g., land use/land cover change (LULCC), white-roofing, etc.) which can be co-associated with other perturbations (Table 5) like those arising from changes to vegetative physical properties (for the LULCC case) which can modify the partitioning of turbulent heat fluxes above and beyond the

520   purely radiatively-driven change (Davin et al., 2007;Bright et al., 2017).

Using a climate efficacy to adjust $RF_{\Delta\alpha}$, however, is not without its drawbacks. A first and obvious drawback is that efficacies are climate model dependent (Hansen et al., 2005;Smith et al., 2020;Richardson et al., 2019). Climate models vary in their underlying physics, which is evidenced by the large spread in CO_2's climate sensitivity across CMIP6 models (Meehl et al.,

525   2020;Zelinka et al., 2020). A second drawback is that climate sensitivities for certain forcing agents like $\Delta\alpha$ are tied to experiments that differ largely in the way forcings have been imposed in time and space. Both drawbacks contribute to large uncertainties in the choice of efficacy for $\Delta\alpha$. The latter drawback is especially problematic since the $\Delta\alpha$ perturbation is often accompanied by perturbations to other surface properties and fluxes (Table 5) having large spatial- and temporal dependencies. The turbulent heat flux perturbations that accompany a net radiative flux change at the surface affect atmospheric temperature

530   and humidity profiles (Bala et al., 2008;Modak et al., 2016;Schmidt et al., 2012;Kravitz et al., 2013), causing the atmosphere to adjust to a new state resulting in a net radiative flux change at TOA that extends beyond the instantaneous shortwave radiative flux change (i.e., $RF_{\Delta\alpha}$).

535   **Table 5. Differences in surface property and flux perturbations between geoengineering-type forcings involving non-vegetative solar radiation management (SRM) and forcings from LULCC, land management change (LMC), or forest management change (FMC). "Δr_a" = change to bulk aerodynamic resistance; "Δr_s" = change to bulk surface resistance; "$\Delta\lambda(E)$" = latent heat flux change from a change to evaporation; "$\Delta\lambda(E+T)$" = latent heat flux change from a change to both evaporation and transpiration; "ΔH" = sensible heat flux change**

Forcing type	Surface property perturbation	Surface flux perturbation
Geoengineering (non-veg. SRM)	$\Delta\alpha$	$\Delta\lambda(E)$, ΔH
LULCC; LMC; FMC	$\Delta\alpha$, Δr_a, Δr_s	$\Delta\lambda(E+T)$, ΔH

540

For example, the efficacy of LULCC forcing across the six studies reviewed by Bright et al. (2015) ranged from 0.5 to 1.02 owed to differences in model set-up (e.g., fixed SST vs. slab vs. dynamic ocean), differences in the spatial extent and magnitude of the imposed LULCC forcing (e.g., historical transient vs. idealized time slice), as well as the LULCC definition (i.e., the

type of LULCC that was included in the study such as only afforestation/deforestation vs. all LULCC). Even when controlling for differences in experimental design (e.g., CMIP protocols), the climate efficacy of historical LULCC has been found to vary considerably in both sign and magnitude (c.f. Figure 8, Richardson et al. 2019), which is more likely attributed to the larger spread in effective radiative forcing (ERF) for LULCC than for CO_2. For instance, Smith *et al.* (2020) report a standard deviation of 6% in the ERF of CO_2 (4×abrupt) across 17 GCMs/ESMs participating in RFMIP in contrast to 175% for LULCC, although it should be kept in mind that the ERF is weak for LULCC thus relative differences become large.

An additional drawback and source of uncertainty underlying efficacies is related to differences in their definition. Differences in definition can stem from either different definitions of RF itself or differences in the definition of the temperature response per unit RF (Richardson et al., 2019;Hansen et al., 2005). Regarding the latter, most base the temperature response for CO_2 on the equilibrium climate sensitivity (ECS) for a CO_2 doubling, although good arguments have been made for using the transient climate response (TCR) instead, particularly for short-lived forcing agents (Marvel et al., 2016;Shindell, 2014). The temperature response for the forcing agent of interest is rarely taken as the equilibrium response although there are some exceptions (e.g. "E_α" in Richardson *et al.* 2019 which is based on climate feedback parameters obtained from ordinary least square regressions). Efficacies are also sensitive to the definition of RF (Richardson et al., 2019;Hansen et al., 2005). For example, the efficacy of sulfate forcing (5×SO_4) has recently been shown to vary from 0.94 to 2.97 depending on whether RF is based on the net radiative flux change at TOA from fixed SST experiments or the instantaneous shortwave flux change at tropopause (Richardson et al., 2019).

Ideally, CO_2-eq. metrics based on the RF concept should be based on an RF definition yielding efficacies approaching unity for a broad range of forcing types. Although there is currently no consensus here, strong arguments have been made for RF definitions based on the net radiative flux change at TOA resulting from fixed SST experiments with GCMs/ESMs (i.e., "F_s" in Hansen et al. 2005; "ERF_{SST}" in Richardson et al. 2019), since such definitions yield efficacies approaching unity for a broad range of forcing types. However, for most $\Delta\alpha$ metric practitioners it is not feasible to quantify atmospheric adjustments and hence the ERF. Efficacies compatible with $RF_{\Delta\alpha}$ (instantaneous ΔSW at TOA) could be the more feasible option for metric calculations, but broad consensus would need to be established first surrounding appropriate efficacy values for different forcing types associated with the $\Delta\alpha$ perturbation (Table 5). This is especially true for forcings involving changes to the biophysical properties of vegetation – such as LULCC, forestry, etc. – since these are constructs representing a seemingly myriad combination of biophysical perturbations acting on non-radiative controls (i.e., Δr_a and Δr_s) of the surface energy balance. Building consensus for efficacies applicable to geoengineering-type forcings where the only physical property perturbed is the surface albedo (e.g., white roofing, sea ice brightening, etc.) would be less challenging since the confounding perturbations to Δr_a and Δr_s and hence to the turbulent heat fluxes are removed. Nevertheless, irrespective of whether broad scientific consensus can be reached surrounding efficacies suitable for $\Delta\alpha$ metrics, additional responsibility would always be imposed on the metric practitioner to ensure that the chosen efficacy aligns with the forcing type underlying the $RF_{\Delta\alpha}$.

8 Discussion

8.1 Summary of merits

In this review, we quantitatively and qualitatively reviewed metrics (methods) to characterize $RF_{\Delta\alpha}$ in terms of a CO_2-equivalent effect. We note that while many metrics exist, none are true "equivalents" to CO_2 due to its unique behavior. The climate effects of the calculated CO_2-eq. emissions should ideally be the same regardless of the mix of forcing agents – including $\Delta\alpha$. However, different forcing agents have different physical properties, and a metric that establishes equivalence with regard to one effect cannot guarantee equivalence with regard to other effects and over extended time periods. Differences among the reviewed $\Delta\alpha$ metrics could be attributed to the different ways of dealing with the time-dependency of RF_{CO2}, which to a large extent was determined by whether a time-dependency was defined for the $\Delta\alpha$ perturbation. When the $\Delta\alpha$ perturbation was assumed to have no time-dependency, as was the case for the *EESF* metric, uncertainties arose from the choice of AF giving a mere snapshot in time of the CO_2 perturbation. For metrics like *GWP* and *TDEE* that explicitly account for the time-dependency of RF_{CO2}, the need to define a time-dependency for $\Delta\alpha$ *a priori* introduces uncertainty owed to the reversible nature of $\Delta\alpha$. Unlike most climate pollutants having standardized perturbation lifetimes determined by the physics of the earth system, the perturbation "lifetime" of $\Delta\alpha$ is tied to a parcel of land and dictated by future anthropogenic activities occurring on that land. Users should strive to be aware of the limitations and caveats of the reviewed $\Delta\alpha$ metrics - defining a $\Delta\alpha$ time-dependency might improve the precision of the CO_2-eq. estimate but not necessarily its accuracy if the future (historical) $\Delta\alpha$ cannot be confidently projected (re-constructed). For instance, application of *EESF* to $\Delta\alpha$ perturbations in dynamic systems (i.e., systems in which $\Delta\alpha$ exhibits large variation over shorter time scales) opens up the risk for grossly mis-characterizing the system, particularly when the chosen $\Delta\alpha$ is not representative of the mean $\Delta\alpha$ of the system under scope (e.g., Fig. 6 B).

Although not applied as a $\Delta\alpha$ metric in the studies we included in our review, our review of *GWP** (Section 6) suggests that it is inferior to *TDEE* as an indicator of future warming when the future time-dependency or "lifetime" of $\Delta\alpha$ is known or defined *a priori* (Fig. 7 B). However, for cases when the future $\Delta\alpha$ is unknown or deemed too uncertain, one could argue that – as a scalar metric – *GWP** has greater scientific merit than *EESF* when applied to step changes in $RF_{\Delta\alpha}$ from the standpoint that CO_2's atmospheric time-dependency is taken explicitly into account. *GWP* – also a scalar metric – has some merit from the standpoint that it is well-known, although scientifically its merits fade when the forcing agent is short-lived (Allen et al., 2018;Lee et al., 2021;Lynch et al., 2020) – as is often the case for $\Delta\alpha$. As a scalar metric that accounts for $\Delta\alpha$'s time-dependency, we deem $\Sigma TDEE$ to have greater scientific merit than *GWP* because it is a better indicator of future warming, which is supported quantitatively by the ΔT reconstructions highlighted in Table 6, based on the $RF_{\Delta\alpha}(t)$ scenarios presented in Figure 7 A.

Table 6. Comparison of future ΔT (global mean) from the $RF_{\Delta\alpha}(t)$ scenarios shown in Figure 7 A reconstructed using *GWP*100 and $\sum_0^{100} TDEE$.

	Actual ΔT at $TH = 100$ yrs., °C	Reconstructed ΔT at $TH = 100$ yrs. using $GWP100$, °C (% of actual)	Reconstructed ΔT at $TH = 100$ using $\sum_0^{100} TDEE$, °C (% of actual)
Scenario A	2.52×10^{-15}	5.25×10^{-16} (21)	2.03×10^{-15} (80)
Scenario B	-1.30×10^{-15}	-6.22×10^{-16} (48)	-1.19×10^{-15} (91)
Scenario C	7.47×10^{-16}	6.16×10^{-16} (82)	7.21×10^{-16} (97)

Although this review has provided needed guidance for choosing appropriate $\Delta\alpha$ metrics according to the context in which they have merit, users should always be mindful that RF_{CO2} and $RF_{\Delta\alpha}$ are not necessarily additive. The global mean temperature may respond differently to identical RFs, and, although there are ways to deal with this discrepancy – either by

615 using ERFs directly in the metric calculation or by adjusting RFs with appropriate efficacy factors. Such approaches require additional modeling tools, which introduces notable additional uncertainties (Section 7). Efficacies for inhomogeneous forcings like $RF_{\Delta\alpha}$ are spatial pattern- and scale-dependent (Shindell et al., 2015), and are sensitive to the climate model set-up and experimental conditions (i.e., how, where, and when $\Delta\alpha$ is imposed in the model). Moreover, efficacies are forcing-type dependent; that is, the forcing signal driving the underlying temperature response may depend on multiple additional

620 perturbations at the surface that are co-associated with $\Delta\alpha$. A good example is LULCC, which perturbs a suite of additional biogeophysical properties affecting surface fluxes (Table 5), some of which resulting in atmospheric feedbacks (or adjustments) that can counteract the $\Delta\alpha$-driven signal (Laguë et al., 2019). Since LULCC represents a broad range of land-based forcings, each of which in turn representing a myriad combination of surface biogeophysical property perturbations, the risk of misapplication of efficacies derived from climate modeling simulations of LULCC is inherently large.

625 **8.2 Research Roadmap**

Research efforts directed towards building a scientific consensus surrounding the most appropriate $RF_{\Delta\alpha}$ estimation method (or model) for use in metric computation would serve to enhance metric transparency and facilitate comparability across studies. Given the ease and efficiency of applying radiative kernels for $RF_{\Delta\alpha}$ calculations, such efforts might entail systematic evaluations and benchmarking of radiative kernels (e.g., as in Kramer et al. (2019)) for $\Delta\alpha$.

630

Reducing uncertainty surrounding the efficacy of $RF_{\Delta\alpha}$ associated with a variety of underlying surface forcing types (i.e., specific LULCC conversions, geoengineering methods, etc.) is paramount to reducing the "additivity" uncertainty (Jones et al., 2013) of RF-based metrics for $\Delta\alpha$. This can be achieved through extending existing climate modeling experimental protocols (e.g., LUMIP, GeoMIP, RFMIP) or by creating new protocols that seek to systematically quantify the sensitivity of

635 the global mean temperature response to variations in the spatial pattern, extent, and magnitude of surface and TOA radiative forcings associated with $\Delta\alpha$.

Research is also needed to examine the relevance of accounting for the climate-carbon feedback in $\Delta\alpha$ metrics, given that such feedback is implicitly included in CO_2's impulse-response function (Gasser et al., 2017). Such research should be mindful of the regional climate response patterns of the various surface forcing types associated with $\Delta\alpha$, and how regional CO_2 sinks are affected in turn by the regional response patterns.

Finally, while not a research need *per se*, a discussion between metric scientists and users/policy makers is needed surrounding three topics (Myhre et al., 2013): i) useful applications; ii) comprehensiveness; and iii) the value of simplicity and transparency. The first involves identifying which application(s) a particular $\Delta\alpha$ metric is meant to serve. We have already shown for instance that the *EESF* metric is not ideal for characterizing dynamic systems. As for comprehensiveness, from a scientific point of view we would ideally wish to be informed about the totality of climate impacts of a $\Delta\alpha$ perturbation at multiple scales (i.e, at both the local and global levels). But a user may often need to aggregate this information, which necessitates trade-offs between impacts at different points in space, between impacts at different points in time, and even between the choice of metric indicator (e.g., *RF* vs. ΔT). Related to the value of simplicity and transparency is the question of whether more complex (yet less transparent) model-based metrics (e.g., those based on *ERF*) are valued by users over simple and more transparent metrics based on analytical formulations. The discussion here should weigh their trade-offs: the former may be more cumbersome to apply or more easily misused, whereas the latter may inadequately capture important physical effects or system dynamics.

8.3 Concluding remarks

For the past several decades, emission metrics have served useful in enabling users or decision makers to quickly perform calculations of the climate impact of GHG emissions. Their common CO_2-equivalent scale has provided flexibility in emissions trading schemes and international climate policy agreements like The Kyoto Protocol. With the advent of the Paris Agreement and a broadened emphasis (Article 4) to include both emissions *and* removals, more attention to land-based mitigation seems likely, and the need for a way to compare albedo and CO_2 on an equivalent scale may increase. This obliges the scientific community to provide users with better tools to do so.

This review has highlighted many of challenges associated with quantifying and interpreting CO_2-equvilanent metrics for $\Delta\alpha$ based on the *RF* concept. A variety of metric alternatives exist, each with their own set of merits and uncertainties depending on the context in which they are applied. The application of metrics always entails user choices, and while some are scientific, others – such as time frame – are policy-related and cannot be informed by science alone. This review has provided guidance to practitioners for choosing a metric with maximum scientific merit and minimum uncertainty according to the specific application context. Going forward, practitioners should always be mindful of the inherent limitations of *RF*-based measures for $\Delta\alpha$, carefully weighing these against the uncertainties of metrics based on impacts further down the cause-effect chain – such as a change in temperature.

Acknowledgements

We acknowledge funding from the Research Council of Norway, grant number 254966. We are grateful for comments and feedback provided by Dr. Gunnar Myhre.

References

675 Akbari, H., Menon, S., and Rosenfeld, A.: Global cooling: increasing world-wide urban albedos to offset CO2, Climatic Change, 94, 275-286, 2009.

Allen, M. R., Fuglestvedt, J. S., Shine, K. P., Reisinger, A., Pierrehumbert, R. T., and Forster, P. M.: New use of global warming potentials to compare cumulative and short-lived climate pollutants, Nature Climate Change, 6, 773-776, 10.1038/nclimate2998, 2016.

680

Allen, M. R., Shine, K. P., Fuglestvedt, J. S., Millar, R. J., Cain, M., Frame, D. J., and Macey, A. H.: A solution to the misrepresentations of CO2-equivalent emissions of short-lived climate pollutants under ambitious mitigation, npj Climate and Atmospheric Science, 1, 16, 10.1038/s41612-018-0026-8, 2018.

685 Bala, G., Duffy, P. B., and Taylor, K. E.: Impact of geoengineering schemes on the global hydrological cycle, Proceedings of the National Academy of Sciences, 105, 7664, 10.1073/pnas.0711648105, 2008.

Bellouin, N., and Boucher, O.: Climate response and efficacy of snow albedo forcings in the HadGEM2-AML climate model. Hadley Centre Technical Note, HCTN82, UK Met Office, 8, 2010.

690

Bernier, P. Y., Desjardins, R. L., Karimi-Zindashty, Y., Worth, D., Beaudoin, A., Luo, Y., and Wang, S.: Boreal lichen woodlands: A possible negative feedback to climate change in eastern North America, Agricultural and Forest Meteorology, 151, 521-528, http://dx.doi.org/10.1016/j.agrformet.2010.12.013, 2011.

695 Betts, R.: Biogeophysical impacts of land use on present-day climate: near-surface termperature change and radiative forcing, Atmospheric Science Letters, 1, 2001.

Betts, R. A.: Offset of the potential carbon sink from boreal forestation by decreases in surface albedo, Nature, 408, 187-190, 2000.
Block, K., and Mauritsen, T.: Forcing and feedback in the MPI-ESM-LR coupled model under abruptly quadrupled CO2, Journal of
700 Advances in Modeling Earth Systems, 5, 676-691, 10.1002/jame.20041, 2014.

Boucher, O., and Reddy, M. S.: Climate trade-off between black carbon and carbon dioxide emissions, Energy Policy, 36, 193-200, 2008.
Boysen, L. R., Lucht, W., Gerten, D., and Heck, V.: Impacts devalue the potential of large-scale terrestrial CO 2 removal through biomass plantations, Environmental Research Letters, 11, 095010, 10.1088/1748-9326/11/9/095010, 2016.

705

Bright, R. M., Cherubini, F., and Strømman, A. H.: Climate Impacts of Bioenergy: Inclusion of Temporary Carbon Cycle and Albedo Change in Life Cycle Impact Assessment, Environmental Impact Assessment Review, 37, 2-11, 2012.

Bright, R. M., Zhao, K., Jackson, R. B., and Cherubini, F.: Quantifying surface albedo changes and direct biogeophysical climate forcings
710 of forestry activities, Global Change Biology, 21, 3246-3266, 2015.

Bright, R. M., Bogren, W., Bernier, P. Y., and Astrup, R.: Carbon equivalent metrics for albedo changes in land management contexts: Relevance of the time dimension, Ecological Applications, 26, 1868-1880, 2016.

715 Bright, R. M., Davin, E., O/'Halloran, T., Pongratz, J., Zhao, K., and Cescatti, A.: Local temperature response to land cover and management change driven by non-radiative processes, Nature Clim. Change, 7, 296-302, 10.1038/nclimate3250, 2017.

Bright, R. M., and O'Halloran, T. L.: Developing a monthly radiative kernel for surface albedo change from satellite climatologies of Earth's shortwave radiation budget: CACK v1.0, Geosci. Model Dev., 12, 3975-3990, 10.5194/gmd-12-3975-2019, 2019.
720

Bright, R. M., Allen, M., Antón-Fernández, C., Belbo, H., Dalsgaard, L., Eisner, S., Granhus, A., Kjønaas, O. J., Søgaard, G., and Astrup, R.: Evaluating the terrestrial carbon dioxide removal potential of improved forest management and accelerated forest conversion in Norway, Global Change Biology, n/a, 10.1111/gcb.15228, 2020.

725 Brovkin, V., Boysen, L., Arora, V. K., Boisier, J. P., Cadule, P., Chini, L., Claussen, M., Friedlingstein, P., Gayler, V., van den Hurk, B. J. J. M., Hurtt, G. C., Jones, C. D., Kato, E., de Noblet-Ducoudré, N., Pacifico, F., Pongratz, J., and Weiss, M.: Effect of Anthropogenic Land-Use and Land-Cover Changes on Climate and Land Carbon Storage in CMIP5 Projections for the Twenty-First Century, Journal of Climate, 26, 6859-6881, 10.1175/JCLI-D-12-00623.1, 2013.

730 Caiazzo, F., Malina, R., Staples, M. D., Wolfe, P., J. ,, Yim, S. H. L., and Barrett, S. R. H.: Quantifying the climate impacts of albedo changes due to biofuel production: a comparison with biogeochemical effects, Environmental Research Letters, 9, 024015, 2014.

Cain, M., Lynch, J., Allen, M. R., Fuglestvedt, J. S., Frame, D. J., and Macey, A. H.: Improved calculation of warming-equivalent emissions for short-lived climate pollutants, npj Climate and Atmospheric Science, 2, 29, 10.1038/s41612-019-0086-4, 2019.

735 Carrer, D., Pique, G., Ferlicoq, M., Ceamanos, X., and Ceschia, E.: What is the potential of cropland albedo management in the fight against global warming? A case study based on the use of cover crops, Environmental Research Letters, 13, 044030, 2018.

Cess, R. D.: Biosphere-Albedo Feedback and Climate Modeling, Journal of the Atmospheric Sciences, 35, 1765-1768, 10.1175/1520-
740 0469(1978)035<1765:BAFACM>2.0.CO;2, 1978.

Chen, L., and Dirmeyer, P. A.: Reconciling the disagreement between observed and simulated temperature responses to deforestation, Nature communications, 11, 202, 10.1038/s41467-019-14017-0, 2020.

745 Cherubini, F., Bright, R. M., and Strømman, A. H.: Site-specific global warming potentials of biogenic CO2 for bioenergy: contributions from carbon fluxes and albedo dynamics, Environmental Research Letters, 7, 045902, 2012.

Ciais, P., Sabine, C., Bala, G., Bopp, L., Brovkin, V., Canadell, J. G., Chhabra, A., DeFries, R., Galloway, J., Heimann, M., Jones, C., Le Quéré, C., Myneni, R. B., Piao, S., and Thornton, P. E.: Carbon and other biogeochemical cycles, in: Climate Change 2013: The Physical
750 Science Basis. Contribution of Working Group I to the Fifth Assessment Report of the Intergovernmental Panel on Climate Change, edited by: Stocker, T. F., Qin, D., Plattner, G.-K., Tignor, M., Allen, S. K., Boschung, J., Nauels, A., Xia, Y., Bex, V., and Midgley, P. M., Cambridge University Press, Cambridge, U.K., and New York, NY, USA, 2013.

Davin, E. L., de Noblet-Ducoudré, N., and Friedlingstein, P.: Impact of land cover change on surface climate: Relevance of the radiative
755 forcing concept, Geophysical Research Letters, 34, L13702, 2007.

de Noblet-Ducoudré, N., Boisier, J.-P., Pitman, A., Bonan, G. B., Brovkin, V., Cruz, F., Delire, C., Gayler, V., van den Hurk, B. J. J. M., Lawrence, P. J., van der Molen, M. K., Müller, C., Reick, C. H., Strengers, B. J., and Voldoire, A.: Determining Robust Impacts of Land-Use-Induced Land Cover Changes on Surface Climate over North America and Eurasia: Results from the First Set of LUCID Experiments,
760 Journal of Climate, 25, 3261-3281, 10.1175/JCLI-D-11-00338.1, 2012.

Denison, S., Forster, P. M., and Smith, C. J.: Guidance on emissions metrics for nationally determined contributions under the Paris Agreement, Environmental Research Letters, 14, 124002, 10.1088/1748-9326/ab4df4, 2019.

765 Donohoe, A., and Battisti, D. S.: Atmospheric and Surface Contributions to Planetary Albedo, Journal of Climate, 24, 4402-4418, 10.1175/2011JCLI3946.1, 2011.

Etminan, M., Myhre, G., Highwood, E. J., and Shine, K. P.: Radiative forcing of carbon dioxide, methane, and nitrous oxide: A significant revision of the methane radiative forcing, Geophysical Research Letters, 43, 12,614-612,623, 10.1002/2016GL071930, 2016.
770 Favero, A., Sohngen, B., Huang, Y., and Jin, Y.: Global cost estimates of forest climate mitigation with albedo: a new integrative policy approach, Environmental Research Letters, 13, 125002, 2018.

Field, L., Ivanova, D., Bhattacharyya, S., Mlaker, V., Sholtz, A., Decca, R., Manzara, A., Johnson, D., Christodoulou, E., Walter, P., and Katuri, K.: Increasing Arctic Sea Ice Albedo Using Localized Reversible Geoengineering, Earth's Future, 6, 882-901,
775 10.1029/2018EF000820, 2018.

Forster, P., Ramaswamy, V., Artaxo, P., Berntsen, T., Betts, R., Fahey, D. W., Haywood, J., Lean, J., Lowe, D. C., Myhre, G., Nganga, J., Prinn, R., Raga, G., Schulz, M., and Van Dorland, R.: Changes in atmospheric consituents and in radiative forcing, in: Climate Change 2007: The Physical Science Basis. Contribution of Working Group I to the Fourth Assessment Report of the Intergovernmental Panel on Climate

780 Change, edited by: Soloman, S., Qin, D., Manning, M., Chen, Z., Marquis, M., Averyt, K. B., Tignor, M., and Miller, H. L., Cambridge University Press, Cambridge, U. K. and New York, NY, USA, 2007.

Fortier, M.-O. P., Roberts, G. W., Stagg-Williams, S. M., and Sturm, B. S. M.: Determination of the life cycle climate change impacts of land use and albedo change in algal biofuel production, Algal Research, 28, 270-281, https://doi.org/10.1016/j.algal.2017.06.009, 2017.

785

Friedlingstein, P., Jones, M. W., O'Sullivan, M., Andrew, R. M., Hauck, J., Peters, G. P., Peters, W., Pongratz, J., Sitch, S., Le Quéré, C., Bakker, D. C. E., Canadell, J. G., Ciais, P., Jackson, R. B., Anthoni, P., Barbero, L., Bastos, A., Bastrikov, V., Becker, M., Bopp, L., Buitenhuis, E., Chandra, N., Chevallier, F., Chini, L. P., Currie, K. I., Feely, R. A., Gehlen, M., Gilfillan, D., Gkritzalis, T., Goll, D. S., Gruber, N., Gutekunst, S., Harris, I., Haverd, V., Houghton, R. A., Hurtt, G., Ilyina, T., Jain, A. K., Joetzjer, E., Kaplan, J. O., Kato, E.,

790 Klein Goldewijk, K., Korsbakken, J. I., Landschützer, P., Lauvset, S. K., Lefèvre, N., Lenton, A., Lienert, S., Lombardozzi, D., Marland, G., McGuire, P. C., Melton, J. R., Metzl, N., Munro, D. R., Nabel, J. E. M. S., Nakaoka, S. I., Neill, C., Omar, A. M., Ono, T., Peregon, A., Pierrot, D., Poulter, B., Rehder, G., Resplandy, L., Robertson, E., Rödenbeck, C., Séférian, R., Schwinger, J., Smith, N., Tans, P. P., Tian, H., Tilbrook, B., Tubiello, F. N., van der Werf, G. R., Wiltshire, A. J., and Zaehle, S.: Global Carbon Budget 2019, Earth Syst. Sci. Data, 11, 1783-1838, 10.5194/essd-11-1783-2019, 2019.

795

Fuglestvedt, J. S., Berntsen, T. K., Godal, O., Sausen, R., Shine, K. P., and Skodvin, T.: Metrics of Climate Change: Assessing Radiative Forcing and Emission Indices, Climatic Change, 58, 267-331, 10.1023/A:1023905326842, 2003.

Fuglestvedt, J. S., Shine, K. P., Berntsen, T., Cook, J., Lee, D. S., Stenke, A., Skeie, R. B., Velders, G. J. M., and Waitz, I. A.: Transport

800 impacts on atmosphere and climate: Metrics, Atmospheric Environment, 44, 4648-4677, https://doi.org/10.1016/j.atmosenv.2009.04.044, 2010.

Gasser, T., Peters, G. P., Fuglestvedt, J. S., Collins, W. J., Shindell, D. T., and Ciais, P.: Accounting for the climate–carbon feedback in emission metrics, Earth Syst. Dynam., 8, 235-253, 10.5194/esd-8-235-2017, 2017.

805

Genesio, L., Bright, R. M., Alberti, G., Peressotti, A., Vedove, G. D., Incerti, G., Toscano, P., Rinaldi, M., Muller, O., and Miglietta, F.: A Chlorophyll-deficient, highly reflective soybean mutant: radiative forcing and yield gaps, Environmental Research Letters, 2020.

Georgescu, M., Lobell, D. B., and Field, C. B.: Direct climate effects of perennial bioenergy crops in the United States, PNAS, 108, 4307-4312, 2011.

810

Guest, G., Bright, R. M., Cherubini, F., and Strømman, A. H.: Consistent quantification of climate impacts due to biogenic carbon storage across a range of bio-product systems, Environmental Impact Assessment Review, 43, 21-30, http://dx.doi.org/10.1016/j.eiar.2013.05.002, 2013.

815 Hansen, J., Sato, M., and Ruedy, R.: Radiative forcing and climate response, Journal of Geophysical Research: Atmospheres, 102, 6831-6864, 10.1029/96JD03436, 1997.

Hansen, J., and Nazarenko, L.: Soot climate forcing via snow and ice albedos, Proceedings of the National Academy of Sciences of the United States of America, 101, 423-428, 10.1073/pnas.2237157100, 2004.

820

Hansen, J., Sato, M., Ruedy, R., Nazarenko, L., Lacis, A., Schmidt, G. A., Russell, G., Aleinov, I., Bauer, M., Bauer, S., Bell, N., Cairns, B., Canuto, V., Chandler, M., Cheng, Y., Del Genio, A., Faluvegi, G., Fleming, E., Friend, A., Hall, T., Jackman, C., Kelley, M., Kiang, N., Koch, D., Lean, J., Lerner, J., Lo, K., Menon, S., Miller, R., Minnis, P., Novakov, T., Oinas, V., Perlwitz, J., Perlwitz, J., Rind, D., Romanou, A., Shindell, D., Stone, P., Sun, S., Tausnev, N., Thresher, D., Wielicki, B., Wong, T., Yao, M., and Zhang, S.: Efficacy of climate forcings,

825 Journal of Geophysical Research: Atmospheres, 110, D18104, 10.1029/2005jd005776, 2005.

Hansen, J. E., Lacis, A., Rind, D., and Russell, G.: Climate Processes and Climate Sensitivity, Geophys. Monogr. Ser., edited by: Hansen, J. E., and Takahashi, T., AGU, Washington, DC, 368 pp., 1984.

830 Heijungs, R., and Guineév, J. B.: An Overview of the Life Cycle Assessment Method – Past, Present, and Future, in: Life Cycle Assessment Handbook, edited by: Curran, M. A., 15-41, 2012.

835 Houghton, J. T., Filho, L. G. M., Bruce, J., Lee, H., Callander, B. A., Haites, E., Harris, N., and Maskell, K.: Radiative forcing of climate change, in: Climate change 1994, Cambridge University Press, Cambridge, U.K., 1995.

Huang, H., Xue, Y., Chilukoti, N., Liu, Y., Chen, G., and Diallo, I.: Assessing global and regional effects of reconstructed land use and land cover change on climate since 1950 using a coupled land-atmosphere-ocean model, Journal of Climate, 1-58, 10.1175/jcli-d-20-0108.1, 2020.

840 IPCC: Climate change 2001: The scientific basis, edited by: Houghton, J., Cambridge University Press, New York, 2001.

Jacobson, M. Z., and Ten Hoeve, J. E.: Effects of Urban Surfaces and White Roofs on Global and Regional Climate, Journal of Climate, 25, 1028-1044, 10.1175/jcli-d-11-00032.1, 2012.

845 Jenkins, S., Millar, R. J., Leach, N., and Allen, M. R.: Framing Climate Goals in Terms of Cumulative CO2-Forcing-Equivalent Emissions, Geophysical Research Letters, 45, 2795-2804, https://doi.org/10.1002/2017GL076173, 2018.

Jones, A. D., Collins, W. D., and Torn, M. S.: On the additivity of radiative forcing between land use change and greenhouse gases, Geophysical Research Letters, 40, 4036-4041, 10.1002/grl.50754, 2013.

850 Joos, F., Roth, R., Fuglestvedt, J. S., Peters, G. P., Enting, I. G., von Bloh, W., Brovkin, V., Burke, E. J., Eby, M., Edwards, N. R., Friedrich, T., Frölicher, T. L., Halloran, P. R., Holden, P. B., Jones, C., Kleinen, T., Mackenzie, F., Matsumoto, K., Meinshausen, M., Plattner, G.-K., Reisinger, A., Segschneider, J., Schaffer, G., Steinacher, M., Strassmann, K., Tanaka, K., Zimmermann, A., and Weaver, A. J.: Carbon dioxide and climate impulse response functions for the computation of greenhouse gas metrics: a multi-model analysis, Atmospheric
855 Chemistry and Physics, 13, 2793-2825, 2013.

Joshi, M., Shine, K., Ponater, M., Stuber, N., Sausen, R., and Li, L.: A comparison of climate response to different radiative forcings in three general circulation models: towards an improved metric of climate change, Climate Dynamics, 20, 843-854, 10.1007/s00382-003-0305-9, 2003.
860

Kramer, R. J., Matus, A. V., Soden, B. J., and L'Ecuyer, T. S.: Observation-Based Radiative Kernels From CloudSat/CALIPSO, Journal of Geophysical Research: Atmospheres, 0, 10.1029/2018JD029021, 2019.

Kravitz, B., Caldeira, K., Boucher, O., Robock, A., Rasch, P. J., Alterskjær, K., Karam, D. B., Cole, J. N. S., Curry, C. L., Haywood, J. M.,
865 Irvine, P. J., Ji, D., Jones, A., Kristjánsson, J. E., Lunt, D. J., Moore, J. C., Niemeier, U., Schmidt, H., Schulz, M., Singh, B., Tilmes, S., Watanabe, S., Yang, S., and Yoon, J.-H.: Climate model response from the Geoengineering Model Intercomparison Project (GeoMIP), Journal of Geophysical Research: Atmospheres, 118, 8320-8332, 10.1002/jgrd.50646, 2013.

Kravitz, B., Rasch, P. J., Wang, H., Robock, A., Gabriel, C., Boucher, O., Cole, J. N. S., Haywood, J., Ji, D., Jones, A., Lenton, A., Moore,
870 J. C., Muri, H., Niemeier, U., Phipps, S., Schmidt, H., Watanabe, S., Yang, S., and Yoon, J. H.: The climate effects of increasing ocean albedo: an idealized representation of solar geoengineering, Atmos. Chem. Phys., 18, 13097-13113, 10.5194/acp-18-13097-2018, 2018.

Laguë, M. M., Bonan, G. B., and Swann, A. L. S.: Separating the Impact of Individual Land Surface Properties on the Terrestrial Surface Energy Budget in both the Coupled and Uncoupled Land–Atmosphere System, Journal of Climate, 32, 5725-5744, 10.1175/jcli-d-18-0812.1,
875 2019.

Lee, D. S., Fahey, D. W., Skowron, A., Allen, M. R., Burkhardt, U., Chen, Q., Doherty, S. J., Freeman, S., Forster, P. M., Fuglestvedt, J., Gettelman, A., De León, R. R., Lim, L. L., Lund, M. T., Millar, R. J., Owen, B., Penner, J. E., Pitari, G., Prather, M. J., Sausen, R., and Wilcox, L. J.: The contribution of global aviation to anthropogenic climate forcing for 2000 to 2018, Atmospheric Environment, 244, 117834,
880 https://doi.org/10.1016/j.atmosenv.2020.117834, 2021.

Lugato, E., Cescatti, A., Jones, A., Ceccherini, G., and Duveiller, G.: Maximising climate mitigation potential by carbon and radiative agricultural land management with cover crops, Environmental Research Letters, 15, 094075, 10.1088/1748-9326/aba137, 2020.

885 Lutz, D., and Howarth, R.: Valuing albedo as an ecosystem service: implications for forest management, Climatic Change, 124, 53-63, 10.1007/s10584-014-1109-0, 2014.

Lynch, J., Cain, M., Pierrehumbert, R., and Allen, M.: Demonstrating GWP*: a means of reporting warming-equivalent emissions that captures the contrasting impacts of short- and long-lived climate pollutants, Environmental Research Letters, 15, 044023, 10.1088/1748-9326/ab6d7e, 2020.

Marvel, K., Schmidt, G. A., Miller, R. L., and Nazarenko, L. S.: Implications for climate sensitivity from the response to individual forcings, Nature Clim. Change, 6, 386-389, 10.1038/nclimate2888 http://www.nature.com/nclimate/journal/v6/n4/abs/nclimate2888.html#supplementary-information, 2016.

Meehl, G. A., Senior, C. A., Eyring, V., Flato, G., Lamarque, J.-F., Stouffer, R. J., Taylor, K. E., and Schlund, M.: Context for interpreting equilibrium climate sensitivity and transient climate response from the CMIP6 Earth system models, Science Advances, 6, eaba1981, 10.1126/sciadv.aba1981, 2020.

Menon, S., Akbari, H., Mahanama, S., Sednev, I., and Levinson, R. M.: Radiative forcing and temperature response to changes in urban albedos and associated CO_2 offsets, Environmental Research Letters, 5, 10.1088/1748-9326/5/1/014005, 2010.

Millar, R. J., Nicholls, Z. R., Friedlingstein, P., and Allen, M. R.: A modified impulse-response representation of the global near-surface air temperature and atmospheric concentration response to carbon dioxide emissions, Atmos. Chem. Phys., 17, 7213-7228, 10.5194/acp-17-7213-2017, 2017.

Modak, A., Bala, G., Cao, L., and Caldeira, K.: Why must a solar forcing be larger than a CO 2 forcing to cause the same global mean surface temperature change?, Environmental Research Letters, 11, 044013, 10.1088/1748-9326/11/4/044013, 2016.

Montenegro, A., Eby, M., Mu, Q., Mulligan, M., Weaver, A. J., Wiebe, E. C., and Zhao, M.: The net carbon drawdown of small scale afforestation from satellite observations, Global and Planetary Change, 69, 195-204, http://dx.doi.org/10.1016/j.gloplacha.2009.08.005, 2009.

Muñoz, I., Campra, P., and Fernández-Alba, A. R.: Including CO2-emission equivalence of changes in land surface albedo in life cycle assessment. Methodology and case study on greenhouse agriculture, International Journal of Life Cycle Assessment, 15, 672-681, 2010.

Myhre, G., Highwood, E. J., Shine, K. P., and Stordal, F.: New estimtes of raditive forcing due to well mixed greenhouse gases, Geophysical Research Letters, 25, 2715-2718, 1998.

Myhre, G., Shindell, D., Bréon, F., Collins, W., Fuglestvedt, J., Huang, J., Koch, D., Lamarque, J., Lee, D., Mendoza, B., and Nakajima, T.: Chapter 8: Anthropogenic and natural radiative forcing, in: Climate Change 2013: The Physical Science Basis. Contribution of Working group I to the Fifth Assement Report of the Integovernmental Panel on Climate Change, edited by: Tignor, K., Allen, M., Boschung, J., Nauels, A., Xia, Y., Vex, V., and Midgley, P., Cambridge University Press, Cambridge, UK and New York, NY, 659-740, 2013.

Mykleby, P. M., Snyder, P. K., and Twine, T. E.: Quantifying the trade-off between carbon sequestration and albedo in midlatitude and high-latitude North American forests, Geophysical Research Letters, 44, 2493-2501, 10.1002/2016GL071459, 2017.

O'Neill, B. C.: The Jury is Still Out on Global Warming Potentials, Climatic Change, 44, 427-443, 10.1023/A:1005582929198, 2000.

O'Neill, B. C., Tebaldi, C., van Vuuren, D. P., Eyring, V., Friedlingstein, P., Hurtt, G., Knutti, R., Kriegler, E., Lamarque, J. F., Lowe, J., Meehl, G. A., Moss, R., Riahi, K., and Sanderson, B. M.: The Scenario Model Intercomparison Project (ScenarioMIP) for CMIP6, Geosci. Model Dev., 9, 3461-3482, 10.5194/gmd-9-3461-2016, 2016.

Pendergrass, A. G., Conley, A., and Vitt, F. M.: Surface and top-of-atmosphere radiative feedback kernels for CESM-CAM5, Earth Syst. Sci. Data, 10, 317-324, 10.5194/essd-10-317-2018, 2018.

Pielke Sr., R. A., Avissar, R., Raupach, M. R., Dolman, A. J., Zeng, X., and Denning, A. S.: Interactions between the atmosphere and terrestrial ecosystems: influence on weather and climate, Global change Biology 4, 461-475, 1998.

Pielke Sr., R. A., Marland, G., Betts, R. A., Chase, T. N., Eastman, J. L., Niles, J. O., Niyogi, D. S., and Running, S. W.: The influence of land-use change and landscape dynamics on the climate system: relevance to climate-change policy beyond the radiative effect of greenhouse gases, Phil. Trans. R. Soc. Lond. A, 360, 1705-1719, 2002.

Pierrehumbert, R. T.: Short-Lived Climate Pollution, Annual Review of Earth and Planetary Sciences, 42, 341-379, 10.1146/annurev-earth-060313-054843, 2014.

Pongratz, J., Reick, C. H., Raddatz, T., and Claussen, M.: Biogeophysical versus biogeochemical climate response to historical anthropogenic land cover change, Geophysical Research Letters, 37, L08702, 10.1029/2010gl043010, 2010.

Richardson, T. B., Forster, P. M., Smith, C. J., Maycock, A. C., Wood, T., Andrews, T., Boucher, O., Faluvegi, G., Fläschner, D., Hodnebrog, Ø., Kasoar, M., Kirkevåg, A., Lamarque, J. F., Mülmenstädt, J., Myhre, G., Olivié, D., Portmann, R. W., Samset, B. H., Shawki, D., Shindell, D., Stier, P., Takemura, T., Voulgarakis, A., and Watson-Parris, D.: Efficacy of Climate Forcings in PDRMIP Models, Journal of Geophysical Research: Atmospheres, 124, 12824-12844, 10.1029/2019JD030581, 2019.

Rogers, J. D., and Stephens, R. D.: Absolute infrared intensities for F-113 and F-114 and an assessment of their greenhouse warming potential relative to other chlorofluorocarbons, Journal of Geophysical Research: Atmospheres, 93, 2423-2428, 10.1029/JD093iD03p02423, 1988.

Schmidt, H., Alterskjær, K., Bou Karam, D., Boucher, O., Jones, A., Kristjánsson, J. E., Niemeier, U., Schulz, M., Aaheim, A., Benduhn, F., Lawrence, M., and Timmreck, C.: Solar irradiance reduction to counteract radiative forcing from a quadrupling of CO_2: climate responses simulated by four earth system models, Earth Syst. Dynam., 3, 63-78, 10.5194/esd-3-63-2012, 2012.

Sciusco, P., Chen, J., Abraha, M., Lei, C., Robertson, G. P., Lafortezza, R., Shirkey, G., Ouyang, Z., Zhang, R., and John, R.: Spatiotemporal variations of albedo in managed agricultural landscapes: inferences to global warming impacts (GWI), Landscape Ecology, 10.1007/s10980-020-01022-8, 2020.

Seneviratne, S. I., Phipps, S. J., Pitman, A. J., Hirsch, A. L., Davin, E. L., Donat, M. G., Hirschi, M., Lenton, A., Wilhelm, M., and Kravitz, B.: Land radiative management as contributor to regional-scale climate adaptation and mitigation, Nature Geoscience, 11, 88-96, 10.1038/s41561-017-0057-5, 2018.

Sherwood, S. C., Bony, S., Boucher, O., Bretherton, C., Forster, P. M., Gregory, J. M., and Stevens, B.: Adjustments in the Forcing-Feedback Framework for Understanding Climate Change, Bulletin of the American Meteorological Society, 96, 217-228, 10.1175/bams-d-13-00167.1, 2015.

Shindell, D. T.: Inhomogeneous forcing and transient climate sensitivity, Nature Clim. Change, 4, 274-277, 10.1038/nclimate2136 http://www.nature.com/nclimate/journal/v4/n4/abs/nclimate2136.html#supplementary-information, 2014.
Shindell, D. T., Faluvegi, G., Rotstayn, L., and Milly, G.: Spatial patterns of radiative forcing and surface temperature response, Journal of Geophysical Research: Atmospheres, 120, 5385-5403, 10.1002/2014JD022752, 2015.

Shine, K., Derwent, R. G., Wuebbles, D. J., and Morcrette, J. J.: Radiative forcing of climate, in: Climate Change: The IPCC Scientific Assessment, edited by: Houghton, J. T., Jenkins, G. J., and Ephraums, J. J., Cambridge University Press, New York, Melbourne, 1990.
Shine, K. P., Cook, J., Highwood, E. J., and Joshi, M. M.: An alternative to radiative forcing for estimating the relative importance of climate change mechanisms, Geophysical Research Letters, 30, 10.1029/2003GL018141, 2003.

Sieber, P., Ericsson, N., and Hansson, P.-A.: Climate impact of surface albedo change in Life Cycle Assessment: Implications of site and time dependence, Environmental Impact Assessment Review, 77, 191-200, https://doi.org/10.1016/j.eiar.2019.04.003, 2019.
Sieber, P., Ericsson, N., Hammar, T., and Hansson, P.-A.: Including albedo in time-dependent LCA of bioenergy, GCB Bioenergy, 12, 410-425, 10.1111/gcbb.12682, 2020.

Singh, B., Guest, G., Bright, R. M., and Strømman, A. H.: Life Cycle Assessment of Electric and Fuel Cell Vehicle Transport Based on Forest Biomass, Journal of Industrial Ecology, 18, 176-186, 10.1111/jiec.12098, 2014.

Smith, C. J., Kramer, R. J., Myhre, G., Forster, P. M., Soden, B. J., Andrews, T., Boucher, O., Faluvegi, G., Fläschner, D., Hodnebrog, Ø., Kasoar, M., Kharin, V., Kirkevåg, A., Lamarque, J.-F., Mülmenstädt, J., Olivié, D., Richardson, T., Samset, B. H., Shindell, D., Stier, P., Takemura, T., Voulgarakis, A., and Watson-Parris, D.: Understanding Rapid Adjustments to Diverse Forcing Agents, Geophysical Research Letters, 45, 12,023-012,031, 10.1029/2018gl079826, 2018.

Smith, C. J., Kramer, R. J., Myhre, G., Alterskjær, K., Collins, W., Sima, A., Boucher, O., Dufresne, J. L., Nabat, P., Michou, M., Yukimoto, S., Cole, J., Paynter, D., Shiogama, H., O'Connor, F. M., Robertson, E., Wiltshire, A., Andrews, T., Hannay, C., Miller, R., Nazarenko, L.,

Kirkevåg, A., Olivié, D., Fiedler, S., Pincus, R., and Forster, P. M.: Effective radiative forcing and adjustments in CMIP6 models, Atmos. Chem. Phys. Discuss., 2020, 1-37, 10.5194/acp-2019-1212, 2020.

Soden, B. J., Held, I. M., Colman, R., Shell, K. M., Kiehl, J. T., and Shields, C. A.: Quantifying Climate Feedbacks Using Radiative Kernels, Journal of Climate, 21, 3504-3520, 10.1175/2007JCLI2110.1, 2008.

Stephens, G. L., O'Brien, D., Webster, P. J., Pilewski, P., Kato, S., and Li, J.-l.: The albedo of Earth, Reviews of Geophysics, 53, 141-163, 10.1002/2014RG000449, 2015.

Susca, T.: Multiscale Approach to Life Cycle Assessment, Journal of Industrial Ecology, 16, 951-962, 10.1111/j.1530-9290.2012.00560.x, 2012a.

Susca, T.: Enhancement of life cycle assessment (LCA) methodology to include the effect of surface albedo on climate change: Comparing black and white roofs, Environmental Pollution, 163, 48-54, https://doi.org/10.1016/j.envpol.2011.12.019, 2012b.

Thompson, M., Adams, D., and Johnson, K. N.: The Albedo Effect and Forest Carbon Offset Design, Journal of Forestry, 107, 425-431, 2009a.

Thompson, M. P., Adams, D., and Sessions, J.: Radiative forcing and the optimal rotation age, Ecological Economics, 68, 2713-2720, 2009b. Wigley, T. M. L.: The Kyoto Protocol: CO2 CH4 and climate implications, Geophysical Research Letters, 25, 2285-2288, https://doi.org/10.1029/98GL01855, 1998.

Zelinka, M. D., Myers, T. A., McCoy, D. T., Po-Chedley, S., Caldwell, P. M., Ceppi, P., Klein, S. A., and Taylor, K. E.: Causes of Higher Climate Sensitivity in CMIP6 Models, Geophysical Research Letters, 47, e2019GL085782, 10.1029/2019GL085782, 2020.

Zhao, K., and Jackson, R. B.: Biophysical forcings of land-use changes from potential forestry activities in North America, Ecological Monographs, 84, 329-353, 10.1890/12-1705.1, 2014.

Zickfeld, K., Eby, M., Matthews, H. D., and Weaver, A. J.: Setting cumulative emissions targets to reduce the risk of dangerous climate change, Proceedings of the National Academy of Sciences, 106, 16129, 10.1073/pnas.0805800106, 2009.